Title: Male age and *Wolbachia* dynamics: Determining how fast and why bacterial densities and cytoplasmic incompatibility strengths vary

Short title: Male age and *Wolbachia* dynamics

Authors: J. Dylan Shropshire[1], Emily Hamant[1], and Brandon S. Cooper[1]

[1]Division of Biological Sciences, University of Montana, Missoula, MT 59812, USA

*Correspondence to:

J. Dylan Shropshire, Missoula, MT, 59801, 423.930.6292, shropxp@gmail.com

ORCID iD: J. Dylan Shropshire (https://orcid.org/0000-0003-4221-2178), Emily Hamant (https://orcid.org/0000-0001-5743-1731), Brandon S. Cooper (https://orcid.org/0000-0002-8269-7731)

Author contributions:

JDS roles: Conceptualization, Data curation, Formal Analysis, Funding acquisition, Investigation, Methodology, Supervision, Validation, Visualization, Writing - original draft, Writing – review & editing. EH roles: Investigation, Validation, Writing – review & editing. BSC roles: Project administration, Conceptualization, Funding acquisition, Supervision, Writing – original draft, Writing – review & editing.

Keywords: aging, immunity, symbiosis, *w*Mel, *w*Ri, *Drosophila*

Abstract

Endosymbiotic *Wolbachia* bacteria infect divergent arthropod and nematode hosts. Many strains cause cytoplasmic incompatibility (CI) that kills uninfected embryos fertilized by *Wolbachia*-modified sperm. Infected embryos are protected from CI, promoting *Wolbachia* spread to high equilibrium frequencies balanced by imperfect maternal transmission. CI strength varies widely in nature and tends to decrease as males age. Understanding the causes of CI-strength variation is crucial to explain *Wolbachia* prevalence in host populations. Here, we investigate how fast and why CI strength decreases with male age in two model systems: *w*Mel in *Drosophila melanogaster* and *w*Ri in *D. simulans*. Average *w*Mel CI strength decreases rapidly (19%/ day), and *w*Ri CI strength decreases slowly (6%/ day) as males age; thus, within three days, *w*Mel-infected males do not cause CI, whereas twelve-day-old *w*Ri-infected males still cause minor, yet significant, CI. We tested if reductions in *Wolbachia* densities or CI gene expression as males age could explain this pattern. Indeed, *w*Ri densities and CI gene expression decrease in testes as males age, but *w*Mel densities and CI gene expression surprisingly increase with male age as CI strength decreases. Phage WO lytic activity and *w*Mel Octomom copy number—an ampliconic gene region that influences *w*Mel proliferation—do not explain age-dependent *Wolbachia* densities. However, the expression of Relish, an essential gene in the *Drosophila* immune deficiency pathway, strongly correlates with *w*Mel densities. Together, these results suggest that testes-wide *Wolbachia* density and CI gene expression are insufficient to explain age-dependent CI strength across strains and that *Wolbachia* density is variably impacted by male age across *Wolbachia*-host associations. We hypothesize that host immunity may underlie variation in age-dependent density dynamics. More broadly, the rapid decline of *w*Mel CI strength during the first week of *D. melanogaster* life likely contributes to *w*Mel frequency variation observed on several continents.

Introduction

Reproductive parasites manipulate host reproduction to facilitate their maternal transmission. These endosymbiotic microbes may kill or feminize males or induce parthenogenesis to bias sex ratios in favor of females [1]. More frequently, reproductive parasites cause cytoplasmic incompatibility (CI) that reduces embryonic viability when aposymbiotic females mate with symbiont-bearing males (**Fig. 1A**) [2]. Females harboring a comparable symbiont are compatible with CI-causing symbiotic males of the same strain, providing symbiont-bearing females a relative advantage that encourages symbiont spread to high frequencies in host populations [3–6]. Divergent *Cardinium* [7], *Rickettsiella* [8], *Mesenet* [9], and *Wolbachia* [10] endosymbionts cause CI. Of these, *Wolbachia* are the most common, infecting 40-65% of arthropod species [11,12]. *Wolbachia* cause CI in at least ten arthropod orders [2], and pervasive CI directly contributes to *Wolbachia* spread and its status as one of the most common endosymbionts in nature.

Within host populations, *Wolbachia* frequencies are governed by their effects on host fitness [13–16], the efficiency of maternal transmission [17–19], and CI strength (% embryonic death) [3,5]. CI strength varies from very weak to very strong and produces relatively low and high infection frequencies, respectively. For example, *w*Yak in *Drosophila yakuba* causes weak CI (~15%) and tends to occur at intermediate and often variable frequencies (~40-88%) in west Africa [18,20]. Conversely, *w*Ri in *D. simulans* causes strong CI (~90%) and occurs at high and stable frequencies (e.g., ~93% globally) [4,21–23]. In *D. melanogaster*, *w*Mel CI strength is relatively weak [24–26], contributing to infection frequencies that vary considerably on multiple continents [27–31]. In contrast, *w*Mel usually causes complete CI (no eggs hatch) in transinfected *Aedes aegypti* mosquitoes [32–35]. Vector control groups use this strong CI to either suppress mosquito populations through the release of *w*Mel-infected males [36–40] or to drive pathogen-blocking *w*Mel to high and stable frequencies to inhibit pathogen spread [32,41,42].

Despite CI's importance for explaining *Wolbachia* prevalence in natural systems and reducing human disease transmission in transinfected mosquito systems, the mechanistic basis of CI-strength variation remains unresolved. Two hypotheses are plausible. First, the bacterial density model predicts that CI is strong when bacterial density is high **(Fig. 1B)** [43]. Indeed, *Wolbachia* densities positively covary with CI strength across *Drosophila*-*Wolbachia* associations [44,45] and with variable CI within strains [33,34,46–52]. Second, the CI gene expression hypothesis predicts that higher CI gene expression contributes to stronger CI **(Fig. 1B)** [53]. In *Drosophila*, two genes (*cifA* and *cifB*) associated with *Wolbachia*'s temperate bacteriophage (WO) induce CI when expressed in testes [53–57], and one gene (*cifA*) rescues CI when expressed in ovaries [56–58]. CI strength covaries with transgenic *cif* expression in *D. melanogaster* [53,57], and natural *cif* expression covaries with CI strength in *Habrobracon* ectoparasitoid wasps [59]. Bacterial density may explain CI strength via *cif* expression but may not perfectly align with CI strength since *Wolbachia* variably express *cifs* across conditions that impact CI strength [53]. Thus, the bacterial density and *cif* expression hypotheses are not mutually exclusive. It remains unknown if *cif* expression is responsible for CI-strength variation and if it covaries with *Wolbachia* density in natural *Drosophila*-*Wolbachia* associations.

If symbiont density is a crucial factor governing CI strength, what governs the change in density? There are several plausible drivers of *Wolbachia* density variation. First, phage WO is a temperate phage capable of cell lysis in some *Wolbachia* strains [59–62]. Lytic phage form particles that burst through the bacterial cell membrane, killing the bacterial host. The phage density model proposes that as phage densities increase, *Wolbachia* densities decrease (**Fig. 1B**) [46]. Temperature-induced phage lysis covaries with lower *Wolbachia* densities and CI strength in some parasitoid wasps [46,59], though it is unknown if phage lysis influences *Wolbachia* densities in any other systems. Second, *w*Mel *Wolbachia* have a unique ampliconic gene region composed of eight genes termed "Octomom" [63,64]. Octomom copy number varies among *w*Mel *Wolbachia* between host generations and positively covaries with *Wolbachia*

densities **(Fig. 1B)**, but effects of Octomom-dependent *Wolbachia* densities on CI have not been investigated. Third, theory predicts that selection favors the evolution of host suppressors [6], as observed for male killing [65,66]. Indeed, CI strength varies considerably across host backgrounds [20,25,35,67], supporting a role for host genotype in CI-strength variation. The genetic underpinnings and mechanistic consequences of host suppression remain unknown, but two models have been proposed [2]. The defensive model suggests that host CI targets diverge to prevent interaction with *cif* products, and the offensive model suggests that host products directly interfere with *Wolbachia* density or the proper expression of *cif* products (e.g., through immune regulation) **(Fig. 1B)**. Only a taxon-restricted gene of *Nasonia* wasps has been functionally determined to contribute to *Wolbachia* density variation [68]; thus considerable work is necessary to uncover host determinants of variation in *Wolbachia* density. Since *Wolbachia* densities significantly contribute to several phenotypes [47,69], investigation of the causes of *Wolbachia* density variation are sorely needed.

CI strength within *Wolbachia*-host systems covaries with several factors, including temperature [25,33,34,46,59], male mating rate [70,71], male development time [72], rearing density [72], nutrition [73], paternal grandmother age [26], and male age [3,16,23,25,70]. Changes in CI strength with male age are particularly notable. Older males cause weaker CI in *w*Mel-infected *D. melanogaster* [25] and *w*Ri-infected *D. simulans* [3,16,23]. Age-dependent CI seems particularly strong for *w*Mel [3,16,23,25], although the precise rates of CI-strength decline have not been estimated. While several factors might contribute to age-dependent CI strength, the precise mechanistic underpinnings of this phenotype remain unknown.

Here, we investigate how fast and why *Wolbachia* densities and CI strengths vary with male age in two model *Wolbachia* that diverged 0.6-6 million years ago [74]: *w*Mel in *D. melanogaster* and *w*Ri in *D. simulans*. First, how fast does CI strength decrease with male age? Second, is *Wolbachia* density consistently correlated with age-related CI strength, as predicted by the bacterial density model? If so, does phage WO lysis, Octomom copy number, or host

immune gene expression correlate with density? Third, does *cif* expression consistently correlate with CI strengths and *Wolbachia* densities, as predicted by the CI gene expression model? This study is the first to test the *cif* expression hypothesis in either system with age and is the highest resolution investigation of *Wolbachia* density variation across age to date. Our results suggest that testes-wide *Wolbachia* densities and *cif* expression alone do not explain age-dependent CI-strength relationships across *Wolbachia*-host associations. While phage WO and Octomom copy number do not covary with the age-dependent *Wolbachia* density variation we observe, immune expression in *D. melanogaster* positively correlates with *w*Mel densities. We discuss how these data contribute to our understanding of the causes of age-dependent CI strength and *Wolbachia* density variation and the consequences for *Wolbachia* prevalence in nature.

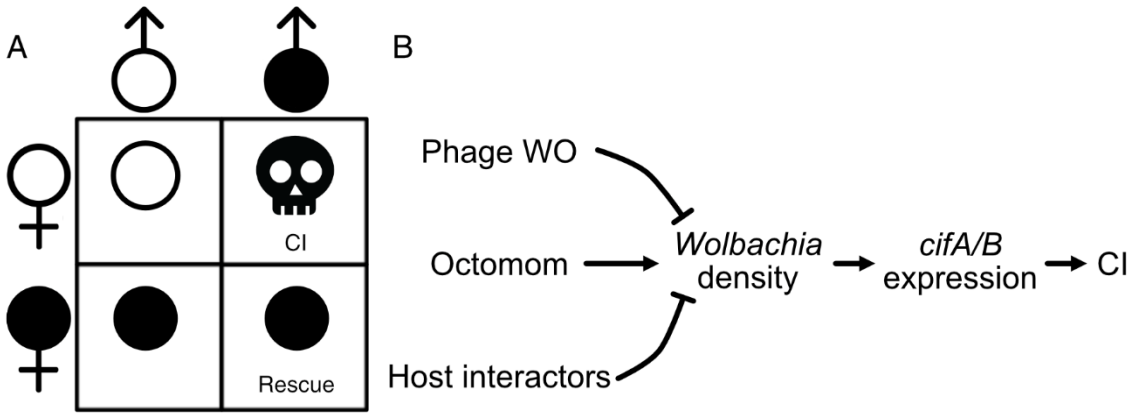

Figure 1. CI crossing relationships and potential causes of CI-strength variation. (A) CI causes embryonic death when infected males (filled symbol) mate with uninfected females (unfilled symbol). Infected females maternally transmit *Wolbachia* and can rescue CI. (B) Schematic representation of factors that putatively impact *Wolbachia* densities, CI gene expression, and CI strength.

Results

How much does CI strength vary with age?

CI manifests as embryonic lethality (**Fig. 1A**). As such, we measured CI strength as the percent of embryos that hatch from a mating pair's clutch of offspring. Our experiments use males of different ages to test the impact of male age on CI strength. Here, we define age as

days since eclosion where males paired with females the day they eclosed are considered 0-days-old. For *w*Mel, we measured CI strength daily across the first three days of male age (**Fig. 2A**) and separately every two days across the first eight days of male age (**Fig. 2B**). This design enabled us to determine the rate of CI decline and the ages where males no longer cause significant CI. Crossing uninfected *D. melanogaster* females and males yields high levels of compatibility (**Fig. 2A**; 95% confidence interval of the mean = 74 - 93%). Young 0-day-old *w*Mel-infected males induce strong CI when mated with uninfected females (95% interval = 9 - 27%). *w*Mel-infected females significantly rescue CI caused by infected 0-day-old males (95% interval = 87 - 92%, *P* = 1.74E-12). Crosses using older 1- (95% interval = 31 - 51%), 2- (95% interval = 53 - 73%), and 3-day-old (95% interval = 69 - 83%) infected males trend toward progressively weaker CI (**Fig. 2A**). Average *w*Mel CI strength decreases daily by 19.3%: 22.8% from 0- to 1-day-old males, 21.8% from 1- to 2-day-old, and 13.4% from 2- to 3-day-old. Crosses between uninfected females and 3-day-old males (95% interval = 69 - 83%) do not cause significant CI, with egg hatch similar to the compatible uninfected (95% interval = 74 - 93%; *P* = 0.35) and rescue (95% interval = 87 - 92%; *P* = 0.19) crosses. This highlights the rapid decline of *w*Mel CI strength with *D. melanogaster* male age.

In the age group that includes older males (**Fig. 2B**), the uninfected cross also yields high compatibility (95% interval = 72 - 88%). 0-day-old infected males cause strong CI when crossed with uninfected females (95% interval = 8 - 15%), and infected females significantly rescue 0-day-old CI (95% interval = 83 - 91%; *P* = 2.51E-12). Older 2- (95% interval = 59 - 73%), 4- (95% interval = 66 - 83%), 6- (95% interval = 76 - 92%), and 8-day-old (95% interval = 77 - 91%) infected males cause weaker CI as males age (**Fig 2B**). CI crosses using 4-day-old or older males do not significantly differ in egg hatch from the compatible uninfected cross (*P* = 1 in all cases). These data suggest that average *w*Mel CI strength decreases by approximately 19.3% each day as *D. melanogaster* males age, but this rate of decrease slows each day, such that CI is no longer statistically detectable once males are 3-days-old.

Next, we assess age-dependent CI in *w*Ri-infected *D. simulans* (**Fig. 2C**). As expected, uninfected *D. simulans* females and males are compatible (95% interval = 74 - 94%). Young 0-day-old *w*Ri-infected males cause strong CI when mated with uninfected females (95% interval = 0 - 1%), and infected females significantly rescue 0-day-old CI (95% interval = 59 - 84%; *P* = 1.83E-10). Older 4- (95% interval = 21 - 39%), 8- (95% interval = 54 - 64%), and 12-day-old (95% interval = 64 - 82%) infected males induce progressively weaker CI as males age. Average *w*Ri CI strength decreases by about 6.0% per day: 29.1% (7.3%/ day) from 0-day-old to 4-day-old males, 29.0% (7.3%/ day) from 4-day-old to 8-day-old, and 14.0% (3.5%/ day) from 8-day-old to 12-day-old. These data support a strong effect of *D. simulans* male age on *w*Ri CI strength, but the daily decrease is more than three times slower than what we observe for *w*Mel CI strength decline as *D. melanogaster* males age.

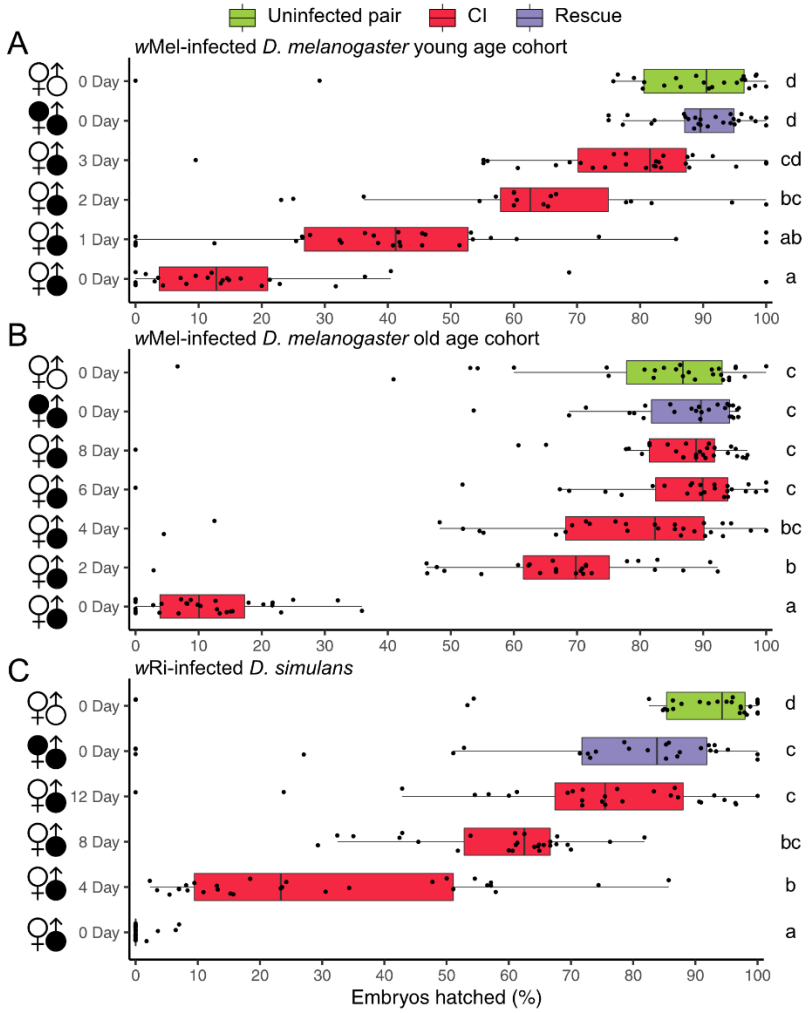

Figure 2. CI strength decreases as males age. (A) Hatch rate displaying CI strength with 0-, 1-, 2-, and 3-day-old *w*Mel-infected *D. melanogaster* males. (B) Hatch rate displaying CI strength with 0-, 2-, 4-, 6-, and 8-day-old *w*Mel-infected *D. melanogaster* males. (C) Hatch rate displaying CI strength with 0-, 4-, 8-, and 12-day-old *w*Ri-infected *D. simulans* males. Filled and unfilled sex symbols represent infected and uninfected flies, respectively. Male age is displayed to the right of the corresponding sex symbol. CI crosses are colored red, rescue crosses are purple, and uninfected crosses are green. Boxplots represent median and interquartile ranges. Letters to the right represent statistically significant differences based on α=0.05 calculated by Kruskal-Wallis and Dunn's test for multiple comparisons between all groups—crosses that do not share a letter are significantly different. *P*-values are reported in **Table S1**. These data demonstrate that CI strength decreases with age in two *Wolbachia*-host associations, and more slowly in *w*Ri-infected *D. simulans*.

What causes CI strength to vary with age?

The bacterial density and CI gene expression hypotheses are both proposed to explain CI-strength variation. These hypotheses predict that *Wolbachia* density and/or *cif* expression

204 positively covary with CI strength. To elucidate the causes of declining CI strength with male
205 age, we test both hypotheses in the context of rapidly declining *w*Mel CI strength and more
206 slowly declining *w*Ri CI strength in *D. melanogaster* and *D. simulans*, respectively.
207
208 *Bacterial density differentially covaries with age between species.*
209 We tested the bacterial density hypothesis by dissecting testes from siblings of flies used
210 in our CI assays above, extracting DNA, and measuring the relative abundance of a single-copy
211 *Wolbachia* gene (*FtsZ*) relative to a single-copy ultraconserved element (UCE) [75] of
212 *Drosophila* via qPCR. We selected a random infected sample from the youngest 0-day-old age
213 group as the reference for all fold change analyses within each experiment. Surprisingly, 0-day-
214 old *D. melanogaster* testes have low *w*Mel density (**Fig. 3A**; 95% interval = 0.53 - 1.01), and
215 older 2- (95% interval = 0.92 - 1.11), 4- (95% interval = 0.96 - 1.72), 6- (95% interval = 1.17 -
216 1.49), and 8-day-old (95% interval = 1.19 - 1.51) infected testes have progressively higher *w*Mel
217 densities (**Fig. 3A**). *w*Mel densities are significantly different among age groups according to a
218 Kruskal-Wallis test (**Fig. 3A**; *P* = 1.1E-03). To test for a correlation between *w*Mel densities and
219 CI strength, we performed Pearson (r_p) and Spearman (r_s) correlations on the relationship
220 between *w*Mel fold change against median hatch rates from the associated age groups. Indeed,
221 *w*Mel densities are significantly positively correlated with decreasing CI strength (**Table S3**; r_p =
222 0.75, *P* = 5.5E-06; r_s = 0.77, *P* = 2.3E-06). *w*Mel densities also covary with age (**Fig. S1**; *P* =
223 0.02) and correlate with decreasing CI strength (**Table S3**; r_p = 0.64, *P* = 7.7E-04; r_s = 0.64, *P* =
224 7.4E-04) in the younger 0-, 1-, 2-, and 3-day-old *D. melanogaster* age group.
225 Next, we tested the bacterial density model in *w*Ri-infected *D. simulans*. In contrast to
226 *w*Mel, *w*Ri-infected 0-day-old (95% interval = 0.82 - 1.36) *D. simulans* testes have the highest
227 *w*Ri densities that consistently decrease in 4- (95% interval = 0.41 - 0.83), 8- (95% interval 0.41
228 - 0.83), and 12-day-old (95% interval = 0.24 - 0.40) testes (**Fig. 3B**). *w*Ri densities are
229 significantly different among *D. simulans* age groups (*P* = 3.9E-04) and are significantly

negatively correlated with decreasing CI strength (**Table S3**; r_p = -0.84, *P* = 2.4E-07; r_s = -0.89, *P* = 6.9E-09).

In conclusion, these data fail to support the bacterial density hypothesis for age-dependent CI-strength variation in *w*Mel-infected *D. melanogaster* but support the hypothesis in *w*Ri-infected *D. simulans*. Thus, testes-wide *Wolbachia* densities alone cannot explain age-dependent CI across *Wolbachia*-host associations, suggesting that other factors must contribute to these patterns. Next, we investigate if *cif* expression covaries with age-dependent CI.

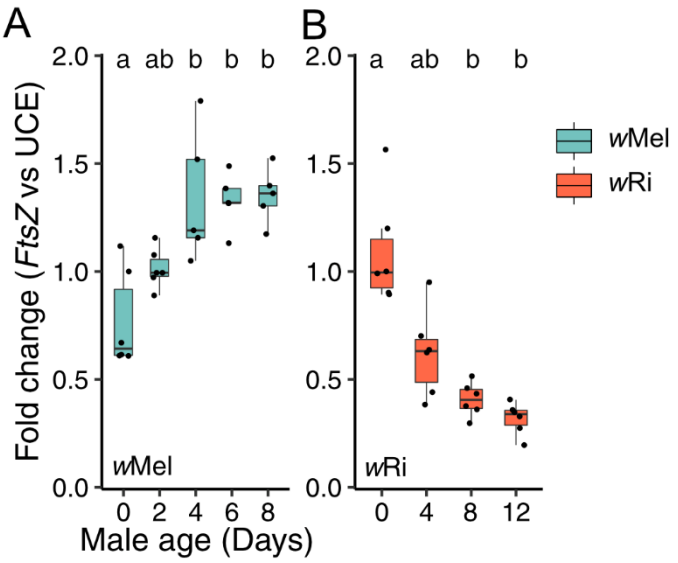

Figure 3. Testing the bacterial density model for CI-strength variation. Fold change across male age for the relative expression of (A) *w*Mel *FtsZ* to *D. melanogaster* UCE and (B) *w*Ri *FtsZ* to *D. simulans* UCE. Letters above data represent statistically significant differences based on α=0.05 calculated by Kruskal-Wallis and Dunn's test for multiple comparisons between all groups—crosses that do not share a letter are significantly different. Fold change was calculated as $2^{-\Delta\Delta cq}$. *P*-values are reported in **Table S1**. These data demonstrate that *Wolbachia* density differentially covaries with age between *Wolbachia*-host associations.

cif expression varies with age, but the direction differs between strains.

cif expression is the proximal mechanistic force hypothesized to control CI-strength variation within *Wolbachia*-host associations [2,53]. *cif* loci are classified into five different

phylogenetic clades called 'Types' [53,76–78]. *w*Mel has a single pair of Type I *cifs,* and *w*Ri has two identical pairs closely related to the *w*Mel copy plus a divergent Type 2 pair [53]. Since *w*Mel density increases as CI strength decreases, we predicted that $cif_{wMel[T1]}$ expression would decrease in age relative to the host. Since *w*Mel densities increase with male age, *w*Mel would need to express $cif_{wMel[T1]}$ at lower levels in older males. Contrary to our first prediction, the relative expression of $cifA_{wMel[T1]}$ to *D. melanogaster* β Spectrin (***βspec***), a *Drosophila* membrane protein with invariable expression with age (see Materials and Methods for details), is low in 0-day-old infected males (95% = 1.1 - 1.6) and consistently increases in 2- (95% interval = 1.5 - 3.2), 4- (95% interval = 1.9 - 2.3), 6- (95% interval = 2.1 - 2.8), and 8-day-old (95% interval = 0.9 - 3.8) testes (**Fig. 4A**). Relative expression of $cifA_{wMel[T1]}$ to ***βspec*** significantly varies across male age (*P* = 8.4E-03) and is significantly positively correlated with decreasing CI strength (**Table S3**; r_p = 0.61, *P* = 6.4E-04; r_s = 0.59, *P* = 9.7E-04). Comparably, relative expression of $cifB_{wMel[T1]}$ to ***βspec*** also significantly increases with male age (**Fig. S2A**; *P* = 7.3E-03). Moreover, analysis of raw quantification cycle (C_q) variation with age supports increased $cifA_{wMel[T1]}$ (**Fig. S2C**; *P* = 3.1E-04) and $cifB_{wMel[T1]}$ (**Fig. S2D**; *P* = 1.1E-03) expression; ***βspec*** C_q does not vary with age (**Fig. S2E**; *P* = 0.1) and *FtsZ* C_q significantly decreases with age (**Fig. S2F**; *P* = 1.3E-04). Thus, we report for the first time that testes-wide *cif* expression is not sufficient to explain CI-strength variation, leading us to reject the hypothesis that testes-wide $cif_{wMel[T1]}$ expression can explain age-dependent *w*Mel CI strength.

However, relative expression of $cifA_{wMel[T1]}$ to *w*Mel *FtsZ* is highest in 0-day-old infected-*D. melanogaster* testes (95% interval = 0.9 - 1.1), and consistently decreases in 2- (95% interval = 0.7 - 0.8), 4- (95% interval = 0.7 - 0.9), 6- (95% interval = 0.6 - 0.7), and 8-day-old (95% interval = 0.4 - 0.9) testes (**Fig. 4B**). Relative expression of $cifA_{wMel[T1]}$ to *w*Mel *FtsZ* significantly varies with age (*P* = 2.9E-03) and is significantly correlated with decreasing CI strength (**Table S3**; r_p = -0.8, *P* = 4.0E-07; r_s = -0.7, *P* = 3.5E-05). Similarly, relative expression of $cifB_{wMel[T1]}$ to *w*Mel *FtsZ* does not significantly covary with age (**Fig. S2B**; P = 0.3), but is significantly

276 correlated with decreasing CI strength (**Table S3**; r_p = -0.42, *P* = 3.7E-02; r_s = -0.46, *P* = 2.2E-
277 02). These data are in line with prior reports that *w*Mel expression of $cifA_{wMel[T1]}$ and $cifB_{wMel[T1]}$
278 decrease as males age [53].

279 We also tested if the relative expression of $cifA_{wMel[T1]}$ to $cifB_{wMel[T1]}$ varied with age.
280 Intriguingly, $cifA/B_{wMel[T1]}$ relative expression does not significantly covary with age (**Fig. 4C**; *P* =
281 0.09), but is positively correlated with decreasing CI strength (**Table S3**; r_p = -0.61, *P* = 1.3E-03;
282 r_s = -0.46, *P* = 0.021). In summary, these data suggest that $cif_{wMel[T1]}$ expression per *w*Mel
283 decreases as males age, that $cifA_{wMel[T1]}$ expression decreases marginally faster than $cifB_{wMel[T1]}$,
284 and that overall $cif_{wMel[T1]}$ expression increases relative to the host as males age and CI strength
285 decreases. This is the first report that CI strength is decoupled from *Wolbachia* densities and *cif*
286 expression in testes.

287 Next, we investigated the *cif* expression hypothesis in *w*Ri. We predicted that $cif_{wRi[T1]}$
288 and/or $cif_{wRi[T2]}$ expression would decrease relative to host expression. Since *w*Ri density
289 decreases with age, *cif* expression per *w*Ri would not need to change to accomplish this shift in
290 relative expression. As predicted, relative expression of $cifA_{wRi[T1]}$ to *D. simulans βspec* is
291 highest in infected 0-day-old (95% interval = 0.7 - 1.7) testes, and declines in 4- (95% interval =
292 0.1 - 0.4), 8- (95% interval = 0.3 - 0.7), and 12-day-old (95% interval = 0.2 - 0.3) testes (**Fig.**
293 **4D**). Relative expression of $cifA_{wRi[T1]}$ to *D. simulans βspec* significantly covaries with age (*P* =
294 1.2E-03) and is significantly correlated with decreasing CI strength (**Table S3**; r_p = -0.76; r_s = -
295 0.88). Similarly, relative expression of $cifB_{wRi[T1]}$ (**Fig. S3A**; *P* = 2.3E-03), $cifA_{wRi[T2]}$ (**Fig. S3C**; *P* =
296 1.9E-03), and $cifB_{wRi[T2]}$ (**Fig. S3E**; *P* = 1.2E-03) to *D. simulans βspec* also decreases with age
297 and each are significantly correlated with decreasing CI strength (**Table S3**). As with *w*Mel-
298 infected *D. melanogaster* testes, relative expression of $cifA_{wRi[T1]}$ to *w*Ri *FtsZ* significantly
299 covaries with male age (**Fig. 4E**; *P* = 4.1E-02) and is significantly correlated with decreasing CI
300 strength (**Table S3**; r_p = -0.47, *P* = 0.032; r_s = -0.47, *P* = 0.033). However, 0- (95% interval = 0.9
301 - 1.2), 4- (95% interval = 0.9 - 1.2), and 8-day-old (95% interval = 0.8 - 1.2) testes have similar

expression patterns, suggesting that expression in 12-day-old (95% interval = 0.5 - 0.9) testes drives this significant difference; however, a Dunn's test was unable to identify significantly different pairs (**Fig. 4E**). Conversely, $cifB_{wRi[T1]}$ (**Fig. S3B**; P = 0.6), $cifA_{wRi[T2]}$ (**Fig. S3D**; P = 0.2), and $cifB_{wRi[T2]}$ (**Fig. S3F**; P = 0.2) expression relative to *w*Ri *FtsZ* did not vary with age or decreasing CI strength (**Table S3**).

Finally, as with *w*Mel, we investigated the relationship between *cifA* and *cifB* expression in *w*Ri across age and found similar results where $cifA_{wRi[T1]}$ expression relative to $cifB_{wRi[T1]}$ expression does not significantly vary with male age (**Fig. 4F**; P = 0.2) but does significantly correlate with decreasing CI strength (**Table S3**; r_p = -0.44, P = 0.045; r_s = -0.46, P = 0.035). Relative expression of $cifA_{wRi[T1]}$ to $cifA_{wRi[T2]}$ expression does not covary with age (**Fig. S3G**; P = 0.6) or decreasing CI strength (**Table S3**; r_p = 0.01, P = 0.96; r_s = -0.05, P = 0.84). Analysis of raw C_q values supports decreasing $cifA_{wRi[T1]}$ (**Fig. S3H**; P = 1.0E-03), $cifB_{wRi[T1]}$ (**Fig. S3I**; P = 8.1E-04), $cifA_{wRi[T2]}$ (**Fig. S3J**; P = 1.8E-03), and $cifB_{wRi[T2]}$ (**Fig. S3K**; P = 1.7E-03) expression with male age; *D. simulans βspec* C_q does not vary with age (**Fig. S3L**; P = 0.6) and *w*Ri *FtsZ* C_q significantly increases with age (**Fig. S3M**; P = 8.9E-04). In summary, cif_{wRi} expression significantly decreases with age in *w*Ri testes, $cifA_{wRi[T1]}$ expression decreases marginally faster than $cifB_{wRi[T1]}$ expression, and there is a small decrease in $cifA_{wRi[T1]}$ expression relative to *w*Ri but other cif_{wRi} loci do not follow similar trends.

In conclusion, we find that *w*Mel *cif* expression does not explain age-dependent CI-strength variation. More specifically, *w*Mel's expression of *cif* genes decreases with age [53], relative *w*Mel and *w*Ri *cifA*-to-*cifB* expression varies marginally with age, and *cif* expression dynamics vary considerably across male age and differ between *w*Mel- and *w*Ri-infected hosts.

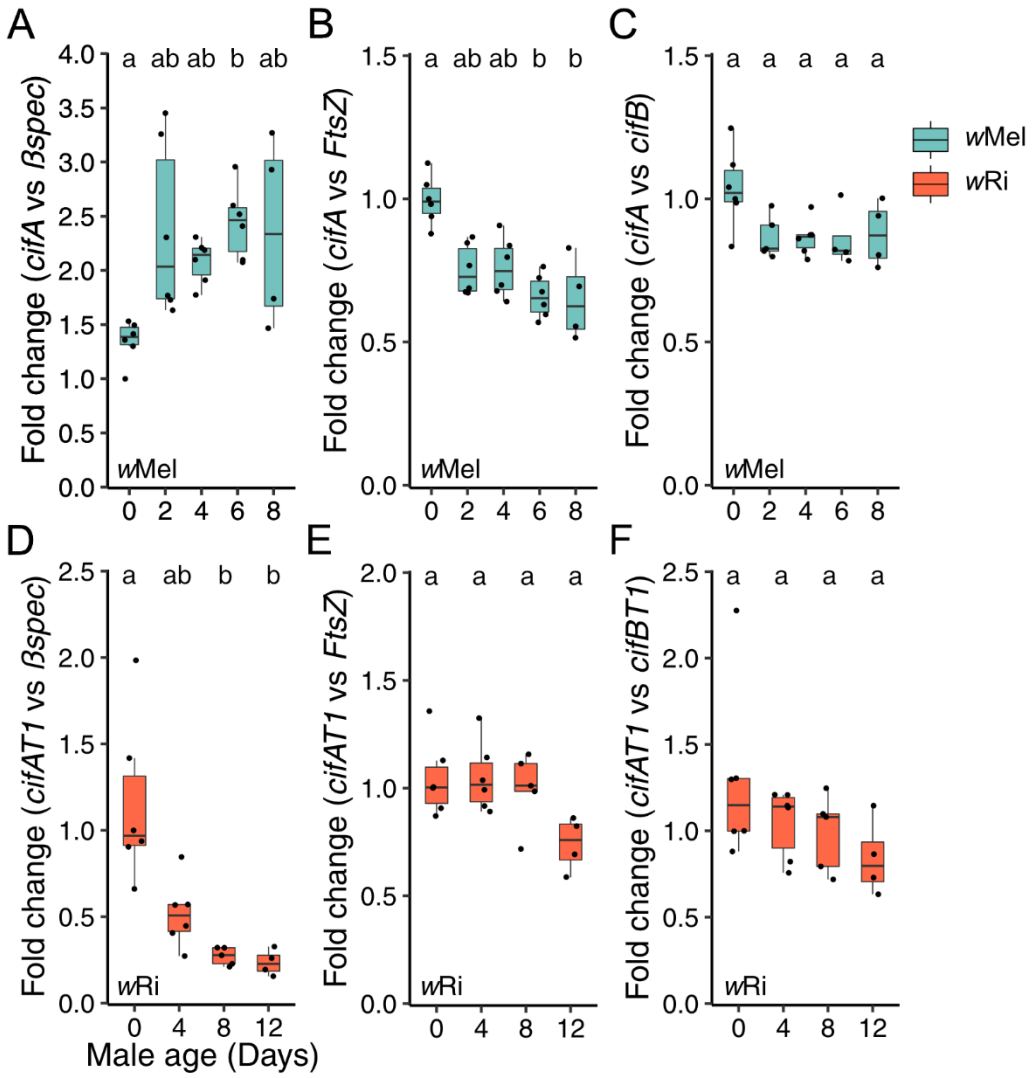

Figure 4. Testing the *cif* expression hypothesis for CI-strength variation. Fold change across male age for the relative expression of (A) $cifA_{wMel[T1]}$ to *D. melanogaster βspec*, (B) $cifA_{wMel[T1]}$ to *w*Mel *FtsZ*, (C) $cifA_{wMel[T1]}$ to $cifB_{wMel[T1]}$, (D) $cifA_{wRi[T1]}$ to *D. simulans βspec*, (E) $cifA_{wRi[T1]}$ to *w*Ri *FtsZ*, and (F) $cifA_{wRi[T1]}$ to $cifB_{wRi[T1]}$. Letters above data represent statistically significant differences based on α=0.05 calculated by Kruskal-Wallis and Dunn's test for multiple comparisons between all groups—crosses that do not share a letter are significantly different. Fold change was calculated as $2^{-\Delta\Delta cq}$. *P*-values are reported in **Table S1**.These data demonstrate that age-dependent *cif* expression is variably related to host expression, that $cif_{wMel[T1]}$ expression decreases per *Wolbachia* with age, and that *cifA/B* relative expression only marginally decreases with age in both systems.

What causes Wolbachia* density *to vary with age?

We find that testes-wide *Wolbachia* density significantly increases with male age in *w*Mel-infected *D. melanogaster* and significantly decreases with male age in *w*Ri-infected *D. simulans*. The causes of age-dependent *Wolbachia* density variation have not been explored. We test three plausible hypotheses. Namely, that phage lytic activity, Octomom copy number, or host immune expression may govern age-dependent *Wolbachia* densities.

Phage density does not covary with age-dependent Wolbachia density.

The phage density model predicts that *Wolbachia* density negatively covaries with phage lytic activity [46]. Since phage lysis corresponds with increased phage copy number [46,59], we tested the phage density model by measuring the relative abundance of phage to *Wolbachia FtsZ* using qPCR. *w*Mel and *w*Ri each harbor a unique set of phage haplotypes: *w*Mel has two phages (WOMelA and WOMelB), and *w*Ri has four (WORiA-C, WORiB is duplicated) [79]. We monitored WOMelA and WOMelB of *w*Mel simultaneously using primers that target homologs present in a single copy in each phage. Conversely, we monitored WORiA, WORiB, and WORiC separately since shared homologs are too diverged to make suitable qPCR primers that match multiple phage haplotypes.

First, we evaluate the phage density model for *w*Mel. We predicted the relative abundance of WOMelA/B to decrease with *D. melanogaster* male age since *w*Mel density increases with age. However, there is no change in WOMelA/B abundance relative to *w*Mel *FtsZ* as males age (**Fig. 5A**; $P = 0.3$), while WOMelA/B abundance relative to *D. melanogaster* UCE increases similar to *w*Mel density (**Fig. S4A**; $P = 3.0E\text{-}04$). Relative phage abundance is not significantly correlated with decreasing *w*Mel CI strength (**Table S3**; $r_p = -0.065$, $P = 0.75$; $r_s = 0.17$, $P = 0.39$). Similarly, WOMelA/B significantly varies with age relative to UCE (**Fig. S4B**; $P = 0.049$) but not *w*Mel *FtsZ* (**Fig. S4C**; $P = 0.15$) in the 0-, 1-, 2-, and 3-day-old age experiment.

Next, we predicted that WORi phage abundance would increase with decreasing *w*Ri densities across *D. simulans* male age if governed by the phage density model. As with *w*Mel in

D. melanogaster, relative WORiB to *w*Ri *FtsZ* abundance does not significantly covary with male age (**Fig. 5B**; *P* = 0.053) or correlate with decreasing CI strength (**Table S3**; r_p = 0.032, *P* = 0.88; r_s = 0.12, *P* = 0.58). Relative WORiB to *D. simulans* UCE abundance increases with age, similar to *w*Ri density (**Fig. S4D**; *P* = 4.4E-04). Comparably, WORiA (**Fig. S4E**; *P* = 0.3) and WORiC (**Fig. S4F**; *P* = 0.4) abundance relative to *w*Ri did not vary with male age. These data suggest that phage WO is unrelated to age-dependent *Wolbachia* density variation in *w*Mel and *w*Ri.

Octomom does not vary with age-dependent wMel density.

The relative abundance of Octomom to *Wolbachia* genes positively covaries with *w*Mel density [64,80]. We tested if Octomom copy number variation correlates with age-dependent *w*Mel density variation using qPCR. Only *w*Mel encodes all eight Octomom genes, and Octomom amplification is rapid and unstable, commonly changing between generations. We found that the relative abundance of an Octomom gene (WD0509) to *w*Mel *FtsZ* does not covary with male age (**Fig. 5C**; *P* = 0.53) or correlate with decreasing CI strength in the older age group (**Table S3**; r_s = -0.19, *P* = 0.36; r_s = 0.1, P = 0.61). Similar results were observed in 0-, 1-, 2-, and 3-day-old *w*Mel-infected males **(Fig. S5; Table S3)**. We conclude that Octomom copy number is unrelated to the age-dependent increase in *w*Mel densities.

Relish expression is positively correlated with age-dependent wMel, but not wRi, densities.

Theory predicts that natural selection favors the evolution of host genes that suppress CI [6]. Manipulation of *Wolbachia* densities is one mechanism that may drive CI suppression [2]. Since the immune system is designed to control bacterial loads, we investigated the role of the host immune system in *Wolbachia* density variation across male age. The immune deficiency (Imd) pathway is broadly involved in defense against gram-negative bacteria like *Wolbachia* [81]. Bacteria activate the Imd pathway by interacting with peptidoglycan recognition proteins

389 which start a signal cascade that results in the expression of the NF-κB transcription factor
390 Relish (*Rel*). Relish then activates antimicrobial peptide production.
391 We predicted that *D. melanogaster* Relish expression and *w*Mel density would be
392 correlated if the Imd pathway is involved in *w*Mel density regulation. Indeed, relative expression
393 of Relish to ***βspec*** is lowest in 0-day-old (95% interval = 0.9 - 1.1) infected testes and
394 consistently increases in 2- (95% interval = 1.1 - 1.8), 4- (95% interval = 1.3 - 1.7), 6- (95%
395 interval = 1.9 - 2.3), and 8-day-old (95% interval = 1.5 - 3.9) testes (**Fig. 5D**). Relative
396 expression of Relish to ***βspec*** significantly varies among age groups (P = 6.1E-4) and is
397 significantly positively correlated with *w*Mel *FtsZ* to ***βspec*** within testes samples (**Fig. 5E**; r_p =
398 0.77, P = 2.5E-06; r_s = 0.87, P = 1.4E-06).
399 Conversely, relative expression of *D. simulans* Relish to ***βspec*** does not significantly
400 covary with age (**Fig. 5F**; P = 0.7), but remains positively correlated with the relative expression
401 of *w*Ri *FtsZ* to ***βspec*** within testes samples according to Pearson, but not Spearman, analyses
402 (**Fig. 5G**; r_p = 0.55, P = 0.012; r_s = 0.13, P = 0.59). In summary, Relish expression is positively
403 correlated with age-dependent *w*Mel densities in *D. melanogaster*, but less so in *w*Ri-infected *D.*
404 *simulans*, supporting a role for the Imd pathway in the regulation of at least *w*Mel density
405 variation. Importantly, since *w*Mel and *w*Ri density are differentially associated with immune
406 expression, Imd activity may represent a novel mechanism separating the age-dependent
407 density dynamics in these systems. These data highlight that age-dependent *Wolbachia* density
408 variation may have multiple mechanistic underpinnings.
409
410

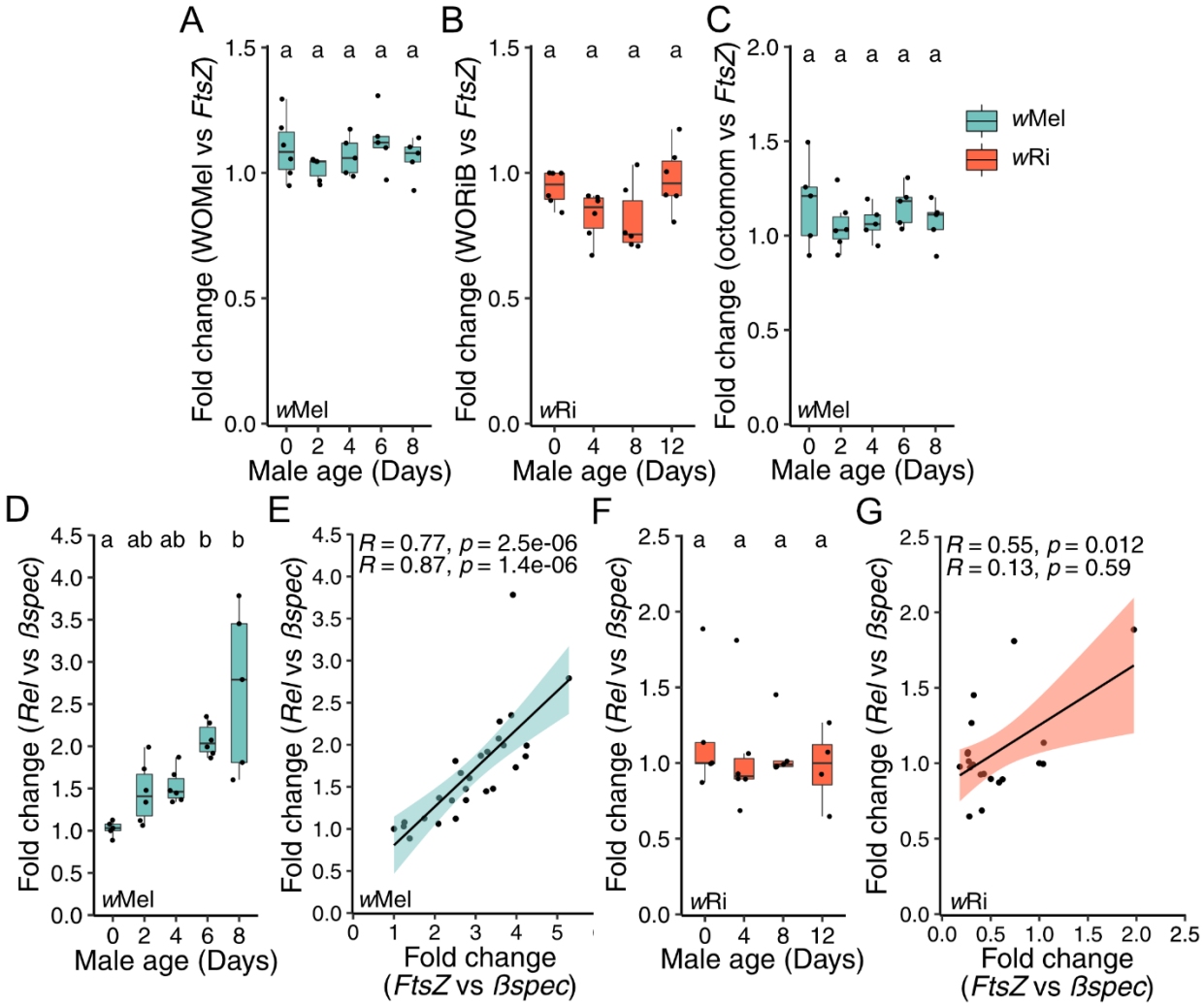

Figure 5. Testing the phage density, Octomom, and host immunity hypotheses for age-dependent *Wolbachia* density variation. Fold change across male age for the relative abundance or expression of (A) WOMelA/B to *w*Mel *FtsZ*, (B) WORiB to *w*Ri *FtsZ*, (C) Octomom gene WD0509 to *w*Mel *FtsZ*, (D) *D. melanogaster Rel* to *Bspec*, and (F) *D. simulans Rel* to *Bspec*. Correlation between the relative expression of *Rel* to *Bspec* and *FtsZ* to *Bspec* for (E) *w*Mel and (F) *w*Ri. Letters above data represent statistically significant differences based on α=0.05 calculated by Kruskal-Wallis and Dunn's test for multiple comparisons between all groups—crosses that do not share a letter are significantly different. (E, G) Pearson (top) and Spearman (bottom) correlations are reported. Fold change was calculated as $2^{-\Delta\Delta cq}$. *P*-values are reported in *Table S1*. These data demonstrate that age-dependent *Wolbachia* densities are not controlled by phage WO lysis or Octomom copy number, but are correlated with *Rel* expression in *D. melanogaster* and less so in *D. simulans*.

Discussion

Within *Wolbachia*-host systems, several factors influence CI strength [25,26,33,34,46,59,70–73], but male age can be particularly impactful [3,16,23,25]. Our results elucidate how fast and why CI strength declines as males age. First, we estimate that CI-strength decreases rapidly for *w*Mel-infected *D. melanogaster* (19%/ day), becoming statistically insignificant when males reach three days old. In contrast, *w*Ri causes intense CI that declines more slowly (6%/ day), resulting in statistically significant CI through at least the first 12 days of *D. simulans* male life. Second, testes-wide *Wolbachia* densities and *cif* expression increase in *w*Mel-infected *D. melanogaster* and decrease in *w*Ri-infected *D. simulans* as males age and CI weakens, indicating that testes-wide bacterial density and CI gene expression cannot fully account for age-dependent CI strength across host-*Wolbachia* associations. Third, while WO phage activity and Octomom copy number cannot explain *Wolbachia* density variation, *D. melanogaster* immune expression covaries with *w*Mel densities, suggesting the host immune system may contribute to age-dependent *Wolbachia* density in *D. melanogaster*, but much less so in *D. simulans*. We discuss how our discoveries inform the basis of age-dependent CI-strength variation, how multiple mechanistic underpinnings likely govern age-dependent *Wolbachia* densities, and how age-dependent CI may contribute to *Wolbachia* frequency variation observed in nature.

Testes-wide Wolbachia density and CI gene expression do not fully explain age-dependent CI-strength variation.

Since CI strength decreases with age for both *w*Mel-infected *D. melanogaster* and *w*Ri-infected *D. simulans*, we predicted that *Wolbachia* densities and *cif* expression would also decrease with age. Indeed, *w*Ri densities and *cif* expression are highest in young males and decrease significantly with age, supporting both the bacterial density and *cif* expression hypotheses for *w*Ri. However, the opposite is true for *w*Mel—both *w*Mel densities and *cif*

451 expression increase with male age as CI strength decreases, indicating that testes-wide
452 *Wolbachia* density and *cif* expression are insufficient to explain age-dependent CI-strength
453 variation in *w*Mel-infected *D. melanogaster*. Despite support that CI strength is linked to
454 *Wolbachia* density and *cif* expression across and within systems [33,34,44–47,53,59], these
455 observations add to a growing body of literature suggesting *Wolbachia* densities in adult testes
456 [26,72] and, for the first time, *cif* expression, are insufficient to explain CI-strength variation
457 broadly. We discuss three hypotheses to explain the disconnect between testes-wide *Wolbachia*
458 density, *cif* expression, and CI strength with male age.

459 First, the localization and density of *Wolbachia* and *cif* products within specific cells in
460 testes may more accurately predict CI strength. Indeed, the proportion of infected spermatocyte
461 cysts covaries with CI strength in natural and transinfected combinations of CI-inducing
462 *Wolbachia* and *D. melanogaster*, *D. simulans*, *D. yakuba*, *D. teissieri*, and *D. santomea* [44,45].
463 Intriguingly, two *w*Ri-infected *D. simulans* strains whose *Wolbachia* cause variable CI did not
464 have different *Wolbachia* densities according to qPCR, but the number of infected sperm cysts
465 covaries with CI between strains [82]. Thus, testes-wide *Wolbachia* densities may not reflect the
466 cyst infection frequency, but it is unknown how generalizable this discrepancy is across or within
467 *Wolbachia*-host associations with variable CI strengths. It seems plausible that while *w*Mel
468 densities increase in the testes as males age, the proportion of infected spermatocytes could
469 decrease. Notably, since *w*Mel infections increase drastically as males age, a considerable shift
470 in localization and density dynamics would be necessary. Microscopy assays are required for
471 future work to test if *Wolbachia* and *cif* localization explains *w*Mel age-dependent CI-strength
472 variation.

473 Second, age-dependent CI may be governed by developmental constraints of CI-
474 susceptibility. For instance, the paternal grandmother age effect, where sons of older virgin
475 females cause stronger CI than sons of younger females, covaries with *Wolbachia* densities in
476 embryos but not in adult males [26]. Intriguingly, temperature-sensitive CI-strength variation in

Cardinium-infected *Encarsia* wasps is also decoupled from symbiont densities, but CI strongly correlates with pupal development time [83,84]. *Cardinium* CI effectors likely have more time to interact with host targets at critical stages of pupal development when slowed by cool temperatures, despite lower *Cardinium* density [83,84]. These studies suggest that sperm are modified in spermatogenesis before adult eclosion, and that variation in symbiont densities during early development can contribute to CI-strength variation. If modified sperm are primarily produced during pupal or larval development, then younger adult males would have a higher proportion of CI-modified sperm than older males in their seminal vesicle since older males continue to produce sperm as adults. Since CI strength decreases faster in *D. melanogaster* than in *D. simulans*, this hypothesis predicts that adult *D. simulans* sperm production is slower and/or that CI modification occurs for an extended time. Functional work is necessary to determine if CI modification is developmentally restricted.

Finally, age-dependent CI may be related to the availability of CI-effector targets with male age and not the abundance of *cif* products. Indeed, the number of genes transcribed by *D. melanogaster* increases from 7,000 in embryos to over 12,000 in adult males, and nearly a third of genes are not expressed until 3rd instar [85]. As adult males age, the number of transcribed genes continues to vary, though less so than during metamorphosis [85]. These data support the possibility that host targets of CI may vary in abundance as males age. However, since transgenic *cif* expression can significantly enhance CI strength above wild-type levels [53], there are circumstances when natural *cif* expression is not high enough to saturate all targets—it is unknown if similar experimental approaches can strengthen age-dependent CI. More work will be necessary to determine the host genes that modify CI and how those factors vary in expression relative to CI strength.

Age-dependent bacterial density covaries with immune expression, not phage or Octomom.

We report a strong relationship between male age and *Wolbachia* densities that differ between systems: densities decrease in *w*Ri-infected *D. simulans* and increase in *w*Mel-infected *D. melanogaster*. These findings add to a growing body of literature reporting age-dependent variation in *Wolbachia* densities across age in different tissues and sexes [44,86], but the basis of this variation remains unexplored. We investigated the cause(s) of this variation for the first time. First, we tested whether phage or Octomom covary with *Wolbachia* densities. Despite prior reports that phage WO of *Nasonia* and *Habrobracon Wolbachia* can regulate temperature-dependent *Wolbachia* densities [46,59] and that Octomom copy number correlates with *w*Mel densities [64,80], we found that neither covaries with age-dependent *Wolbachia* densities in testes.

We next asked whether host genes regulate age-dependent *Wolbachia* densities. *Wolbachia* are gram-negative bacteria and encode the genes necessary to synthesize peptidoglycan, which can activate the host Imd pathway to produce antimicrobial peptides (AMPs) for immune defense [87,88]. Thus, host immune genes were attractive candidates for the regulation of *Wolbachia* densities. Here, we report that Relish expression, which activates AMP production in the Imd pathway [81], increases with *D. melanogaster* male age and strongly correlates with increased *w*Mel densities. Conversely, Relish does not vary with *D. simulans* male age and is only very weakly correlated with *w*Ri densities. Relish expression is the only factor we investigated that differentiates the density dynamics of these strains and is an exciting candidate gene for host manipulation of *Wolbachia* density dynamics. To our knowledge, this is the first report that host immunity covaries with *Wolbachia* density. We propose two non-exclusive hypotheses to explain the relationship between *w*Mel densities and Relish expression.

First, *w*Mel rapidly proliferates as males age and elicit an immune response proportional to their infection density. Since established *Wolbachia* are bound in host-derived membranes [89], *w*Mel may largely evade the host immune response [11]. Indeed, AMP gene expression only covaries with infection state in transinfected [90–93], and not established infections [94–

97], suggesting that *Wolbachia* can be targeted by Imd but adapt to avoid its effects. Thus, the *Drosophila* immune system may be attempting, but unable, to control age-dependent *Wolbachia* densities. This hypothesis does not explain differences between *w*Mel and *w*Ri densities since it assumes age-dependent *w*Mel densities increase independent of Imd expression. Thus, an alternative mechanism unrelated to immune expression may contribute to variation in age-dependent *Wolbachia* densities across species.

Second, Imd expression increases independent of *Wolbachia* infection but impacts *Wolbachia* densities. Indeed, aging in *D. melanogaster* is associated with increased expression of AMPs, Relish, and other immune genes [98–104], and age covaries with increased gut microbial loads [98–100,105–107]. Why gut bacterial loads increase with *D. melanogaster* age remains unknown; but age-dependent immune expression may damage the epithelium, lead to dysbiosis through differential effects on gut microbial members, alter gut tissue renewal and differentiation, and/or cause cellular inflammation [81,108]. To our knowledge, we report the first case where endosymbiont densities increase with age-dependent immune expression, suggesting that the cause(s) of age-dependent bacterial proliferation apply to more than gut microbes. Such age-dependent immune expression may be host restricted since Relish expression was essentially invariable with age in *D. simulans* males and only weakly correlated with *w*Ri densities. Functional and cell biological assays are needed to reinforce the relationship between host immunity, other novel host factors, and age-dependent *Wolbachia* densities. Mapping additional host factors that modulate *Wolbachia* densities will be particularly useful.

Age-dependent CI strength could contribute to *Wolbachia* frequency variation in nature.

We can consider our estimates of age-dependent CI strength in the context of an idealized discrete-generation model of *Wolbachia* frequency dynamics first proposed by Hoffmann et al. (1990). This model incorporates imperfect maternal transmission (μ), *Wolbachia* effects on host fitness (F), and the proportion of embryos that hatch in a CI cross relative to

555 compatible crosses (*H*) [3]. Across all experiments, CI strength (s_h = 1 - *H*) progressively
556 decreases as males age (**Table S2**): *w*Mel CI strength decreases quickly (Day 0 s_h = 0.860; Day
557 8 s_h = -0.007) and *w*Ri CI strength decreases relatively slowly (Day 0 s_h = 0.991; Day 8 s_h =
558 0.244). Small negative values of s_h indicate that the CI cross has a slightly higher egg hatch
559 than the compatible crosses.

560 *w*Ri occurs globally at high and relatively stable infection frequencies, consistent with
561 generally strong CI [4,22], while *w*Mel varies in frequency on several continents. In eastern
562 Australia, *w*Mel frequencies range from ~90% in the tropical north to ~30% in the temperate
563 south [30]. While the factors that maintain this cline are unresolved, mathematical modeling
564 suggests clinal differences in CI strength likely contribute [30]. For example, CI must be
565 essentially nonexistent (s_h << 0.05) to explain relatively low *w*Mel frequencies observed in
566 temperate Australia, assuming little imperfect transmission (μ = 0.01 - 0.026) [109]. Conversely,
567 with μ = 0.026 and similarly low-to-nonexistent CI ($s_h \leq 0.055$), large and positive *w*Mel effects
568 on host fitness (*F* ~ 1.3) are required to explain higher *w*Mel frequencies observed in the tropics.
569 Though, explaining higher tropical frequencies becomes easier with stronger CI ($s_h > 0.05$) or
570 more reliable *w*Mel maternal transmission ($\mu < 0.026$) (Kriesner et al. 2016).

571 So what is *w*Mel CI strength in nature? Field-collected males from near the middle of the
572 Australian cline to the northern tropics cause very weak (s_h ~ 0.05) to no CI (Hoffmann et al.
573 1998). These, and other data from the middle of the cline [25], led Kriesner et al. (2016) to
574 conjecture that the plausible range of s_h in subtropical/tropical Australian populations is s_h = 0 -
575 0.05, but < 0.1. In our study, only 6- (s_h = -0.006) and 8-day-old (s_h = -0.007) *w*Mel-infected
576 males exhibited CI weaker than s_h = 0.1, suggesting that field-collected males causing little or
577 no CI [109] are older than 4 days. Though, interactions among male age, temperature,
578 remating, and other factors likely contribute to weaker CI in younger males
579 [25,33,34,46,59,70,71]. Future analyses aimed at disentangling the contributions of male age
580 and other factors to CI-strength variation are sorely needed. These estimates, along with

581 estimates of *Wolbachia* transmission rate variation across genetic and abiotic contexts [18], are
582 ultimately required to better understand *Wolbachia* frequency variation in host populations
583 [18,20,30,110,111].
584
585 ***Conclusions.***
586 Our results highlight that testes-wide *Wolbachia* densities and *cif* expression are
587 insufficient to explain age-dependent CI strength and that no single mechanism is likely to
588 explain age-dependent *Wolbachia* densities. While age-dependent CI strength in *w*Ri aligns with
589 the bacterial density and CI gene expression hypotheses without the need to consider other
590 factors, *w*Mel CI strength cannot be explained by either of these hypotheses. We propose that
591 localization, development, and/or host genetic variation contribute to this relationship. Moreover,
592 *w*Mel densities increase and *w*Ri decrease as their respective hosts age. Neither phage WO nor
593 Octomom explain age-dependent *Wolbachia* density, but variation in these systems covaries
594 with the expression of the immune gene Relish. This represents the first report that the host
595 immune system may contribute to variation in *Wolbachia* density in a natural *Wolbachia*-host
596 association. This work motivates an extensive analysis of *Wolbachia* and *cif* expression in the
597 context of localization and development, and a thorough investigation of the relationship
598 between host genes and *Wolbachia* density and CI phenotypes. Finally, Incorporating the age-
599 dependency of CI into future modeling efforts may help improve our ability to explain temporally
600 and spatially variable *Wolbachia* infection frequencies, as incorporating temperature effects on
601 *w*Mel-like *Wolbachia* transmission has [18,20,112]. Ultimately this will help explain *Wolbachia's*
602 status as the most prevalent endosymbionts in nature.
603

Materials and Methods

Fly lines

All fly lines used in this study are listed in **Table S4**. Uninfected flies were derived via tetracycline treatment in prior studies [14,53]. Tetracycline cleared lines were used in experiments over a year after treatment, avoiding the effects of antibiotic treatment on mitochondria [113]. We regularly confirmed infection status by using PCR to amplify the *Wolbachia* surface protein (*wsp*). An arthropod-specific 28S rDNA was also amplified and served as a control for DNA quality [20,74]. DNA was extracted for infection checks using a squish buffer protocol. Briefly, flies were homogenized in 50 uL squish buffer per fly (100mL 1M Tris-HCL, 0.0372g EDTA, 0.1461g NaCl, 90 mL H_2O, 150uL Proteinase K), incubated at 65ºC for 45m, incubated at 94ºC for 4m, centrifuged for 2m, and the supernatant was used immediately for PCR.

Fly care and maintenance

Flies were reared in vials with 10mL of food made of cornmeal (32.6%), dry corn syrup (32%), malt extract (20.6%), inactive yeast (7.8%), soy flour (4.5%), and agar (2.6%). Fly stocks were maintained at 23ºC between experiments. Flies used for virgin collections were reared at 25ºC, virgin flies were stored at 25ºC, and experiments were performed at 25ºC. Flies were always kept on a 12:12 light:dark cycle. Flies were anesthetized using CO_2 for virgin collections and dissections. During hatch-rate assays, flies were mouth aspirated between vials.

Hatch-rate assays

CI manifests as embryonic death. We measured CI as the percentage of embryos that hatch into larva. Flies used in hatch rates were derived from vials where flies were given ~24hr to lay to control for rearing density [72]. In the morning, virgin 6-8 day females were added

individually to vials containing a small ice cream spoon filled with fly food. Spoon fly food was prepared as described above, but with blue food coloring added, 0.1g extra agar per 100mL of food, and fresh yeast smeared on top. After 4-5hr of acclimation, a single virgin male was added to each vial. The age of virgin males varied by experiment and cross. Paternal grandmother age was not controlled, but paternal grandmothers were non-virgin when setting up vials for fathers. Since *Wolbachia* densities associated with older paternal grandmothers are reduced upon mating [26], we do not expect variation in paternal grandmother *Wolbachia* densities across experiments or conditions. Vials with paired flies were incubated overnight at 25ºC. Flies were then aspirated into new vials with a fresh spoon. Vials were incubated for another 24hr before flies were removed via aspirating. Embryos were counted on spoons immediately after flies were removed. After 48hr, the number of remaining unhatched eggs were counted. The percentage of embryos that hatched was calculated.

Relative abundance assays

Siblings from hatch-rate assays were collected for DNA extractions. Virgin males were anesthetized and testes were dissected in chilled phosphate-buffered saline (PBS). Five pairs of testes were placed into a single 1.5mL Eppendorf tube and stored at -80ºC until processing. All tissue was collected the day after the hatch-rate setup. Tissue was homogenized using a pestle, and the DNeasy Blood and Tissue kit (Qiagen) was used to extract and purify DNA.

qPCR was used to measure the relative abundance of the host, *Wolbachia*, phage WO, and Octomom products. Samples were tested in triplicate using Powerup SYBR Green Master Mix (Applied Biosystems), which contains a ROX passive reference dye. Unless otherwise noted, all primers were designed using Primer3 v2.3.7 in Geneious Prime [114]. Host primers target an ultraconserved element (UCE) *Mid1* identified previously [75]. Phage genes were also identified from prior works [79]. Primers for *w*Mel's phages target both WOMelA (WD0288) and WOMelB (WD0634), while those for *w*Ri are unique to a single phage haplotype. WORiA,

WORiB, and WORiC were measured with *w*Ri_012460, *w*Ri_005590/*w*Ri_010250, and *w*Ri_006880 primers, respectively. Only *w*Mel has all eight Octomom genes (WD0507-WD0514) [63]. We measured *w*Mel Octomom copy number using primers targeting WD0509. Primer sequences and PCR conditions are listed in **Table S5**. Fold difference was calculated as $2^{-\Delta\Delta Ct}$ for each comparison. A random sample in the youngest age group was selected as the reference.

Gene expression assays

Siblings from hatch-rate assays were collected for RNA extractions. Virgin males were anesthetized, and testes were dissected in chilled RNase-free PBS. Fifteen pairs of testes were placed into a single 2mL tube with 200 uL of Trizol and four 3 mm glass beads. Tissue was kept on ice between dissections. Samples were then homogenized using a TissueLyser II (Qiagen) at 25Hz for 2m, centrifuged, and stored at -80^{o}C until processing. All tissue was collected the day after the hatch-rate setup.

Samples were thawed, 200uL of additional Trizol was added, and tissue was further homogenized using a TissueLyser II at 25Hz for 2m. RNA was extracted using the Direct-Zol RNA Miniprep kit (Zymo Research) following the manufacturer's recommendations, but with an extra wash step. On-column DNase treatment was not performed. The 'rigorous' treatment protocol from the DNA-free kit (Ambion) was used to degrade DNA in RNA samples. Samples were confirmed DNA-free using PCR and gel electrophoresis for an arthropod-specific 28S rDNA [20,74]. The Qubit RNA HS Assay Kit (Invitrogen) was used to measure RNA concentration. Samples within an experiment were diluted to the same concentration. RNA was converted to cDNA using SuperScript IV VILO Master Mix (Invitrogen) with either 200ng or 500ng of total RNA per reaction depending on the experiment. qRT-PCR was performed using 1ng of cDNA per reaction using Powerup SYBR Green Master Mix (Applied Biosystems). All samples were tested in triplicate.

Primers for expression included host reference, *Wolbachia* reference, *cif*, and host immune genes. Primers to *Drosophila* genes for qRT-PCR were selected from FlyPrimerBank [115]. Since *Drosophila* expression patterns change with age [85], a host gene that is invariable with male age was selected to act as a reference gene for relative expression analyses. We selected an invariable gene using the *Drosophila* Gene Expression Tool (DGET) to retrieve modENCODE gene expression data for ribosome and cytoskeletal genes [116]. DGET reports expression as Reads Per Kilobase of transcript, per million mapped reads (RPKM), and included data for adult males 1, 5, and 30 days after eclosion. β-spec (1 Day = 81 RPKM, 5 Day = 80, 30 Day = 79) was selected because it is largely invariable across age. Our results confirm invariable expression across male age (**Fig. S2E**; **Fig. S3L**). *D. melanogaster* and *D. simulans* are identical across *βspec* primer binding sequences. All other primers were designed using Primer3 in Geneious Prime [114] and are listed in **Table S5**. Fold difference was calculated as $2^{-\Delta\Delta Ct}$ for each comparison. A random sample in the youngest age group was selected as the reference.

Statistical analyses

All statistics were performed in R [117]. Hatch rate, relative abundance, and expression assays were analyzed using a Kruskal-Wallis followed by a Dunn's multiple comparisons test. Kruskal-Wallis and Dunn's *P*-values are reported in **Table S1**. Correlations between hatch rate and expression or relative abundance measures were performed using Pearson and Spearman correlations in GGPubR [118]. Correlation statistics are reported in **Table S3**. 95% confidence intervals were calculated using the classic MeanCI function in DescTools [119]. 95% BCa intervals were calculated using boot.ci in boot [120]. Samples with fewer than ten embryos laid were excluded from hatch-rate analyses. Samples with a C_q standard deviation exceeding 0.4 between triplicate measures were excluded from qPCR and qRT-PCR analyses. Figures were

706 created using GGPlot2 [121], and figure aesthetics were edited in Affinity Designer 1.8 (Serif
707 Europe, Nottingham, UK).
708
709 ***Data availability***
710 All data are made publicly available in the supplement of this manuscript.
711
712 **Acknowledgments**
713 We thank Michael Turelli for helpful feedback and members of the Cooper Lab for
714 providing assistance throughout this study: Will Conner for help identifying phage gene targets
715 for qPCR, Mike Hague for support with BCa estimates of *H*, Kelley Van Vaerenberghe and John
716 Statz for review of earlier versions of the manuscript, and Tim Wheeler for assisting in the
717 laboratory. This work was supported by a National Institutes of Health R35 GM124701 to BSC
718 and a National Science Foundation Postdoctoral Research Fellowship DBI-2010210 to JDS.
719 Any opinions, findings, conclusions, or recommendations expressed in this material are those of
720 the authors(s) and do not necessarily reflect the views of the National Institutes of Health or the
721 National Science Foundation.
722

References

1. Kaur R, Shropshire JD, Cross KL, Leigh B, Mansueto AJ, Stewart V, et al. Living in the endosymbiotic world of *Wolbachia*: A centennial review. Cell Host & Microbe. 2021;0. doi:10/gkbpkz

2. Shropshire JD, Leigh B, Bordenstein SR. Symbiont-mediated cytoplasmic incompatibility: what have we learned in 50 years? eLife. 2020;9: e61989. doi:10/ghgtbv

3. Hoffmann A, Turelli M, Harshman L. Factors affecting the distribution of cytoplasmic incompatibility in *Drosophila simulans*. Genetics. 1990;126: 933–948. doi:10/gkbpn6

4. Kriesner P, Hoffmann AA, Lee SF, Turelli M, Weeks AR. Rapid sequential spread of two *Wolbachia* variants in *Drosophila simulans*. PLOS Pathogens. 2013;9: e1003607. doi:10/gbdssd

5. Hoffmann A, Turelli M. in Influential Passengers: Inherited Microorganisms and Arthropod Reproduction. Oxford University Press; 1997. pp. 42–80.

6. Turelli M. Evolution of incompatibility-inducing microbes and their hosts. Evolution. 1994;48: 1500–1513. doi:10/gkbppg

7. Hunter MS, Perlman SJ, Kelly SE. A bacterial symbiont in the Bacteroidetes induces cytoplasmic incompatibility in the parasitoid wasp *Encarsia pergandiella*. Proceedings of the Royal Society B: Biological Sciences. 2003;270: 2185–2190. doi:10/bdkbg6

8. Rosenwald LC, Sitvarin MI, White JA. Endosymbiotic Rickettsiella causes cytoplasmic incompatibility in a spider host. Proceedings of the Royal Society B: Biological Sciences. 2020;287: 20201107. doi:10/gkbppq

9. Takano S, Gotoh Y, Hayashi T. "Candidatus *Mesenet longicola*": Novel Endosymbionts of *Brontispa longissima* that Induce Cytoplasmic Incompatibility. Microbial Ecology. 2021. doi:10/gkbptr

10. Yen JH, Barr AR. The etiological agent of cytoplasmic incompatibility in *Culex pipiens*. Journal of Invertebrate Pathology. 1973;22: 242–250. doi:10/dznftn

11. Zug R, Hammerstein P. Still a host of hosts for *Wolbachia*: analysis of recent data suggests that 40% of terrestrial arthropod species are infected. PLOS ONE. 2012;7: e38544. doi:10/f32jn3

12. Weinert LA, Araujo-Jnr EV, Ahmed MZ, Welch JJ. The incidence of bacterial endosymbionts in terrestrial arthropods. Proc R Soc B. 2015;282: 20150249. doi:10/ggjc2f

13. Brownlie JC, Cass BN, Riegler M, Witsenburg JJ, Iturbe-Ormaetxe I, McGraw EA, et al. Evidence for metabolic provisioning by a common invertebrate endosymbiont, *Wolbachia pipientis*, during periods of nutritional stress. PLoS Pathog. 2009;5: e1000368. doi:10/cchz5m

14. Hague MTJ, Caldwell CN, Cooper BS. Pervasive Effects of *Wolbachia* on Host Temperature Preference. mBio. 2020;11. doi:10/ghxpgn

15. Teixeira L, Ferreira A, Ashburner M. The bacterial symbiont *Wolbachia* induces resistance to RNA viral infections in *Drosophila melanogaster*. PLoS Biol. 2008;6: e2. doi:10/fkgg7f

16. Weeks AR, Turelli M, Harcombe WR, Reynolds KT, Hoffmann AA. From parasite to mutualist: Rapid evolution of *Wolbachia* in natural populations of *Drosophila*. PLOS Biology. 2007;5: 997–1005. doi:10/bnhxkf

17. Carrington LB, Lipkowitz JR, Hoffmann AA, Turelli M. A re-examination of *Wolbachia*-induced cytoplasmic incompatibility in California *Drosophila simulans*. PLOS One. 2011;6: e22565. doi:10/bj2df2

18. Hague MTJ, Mavengere H, Matute DR, Cooper BS. Environmental and Genetic Contributions to Imperfect *w*Mel-Like *Wolbachia* Transmission and Frequency Variation. Genetics. 2020;215: 1117–1132. doi:10/gkbppm

19. Serbus LR, Sullivan W. A cellular basis for *Wolbachia* recruitment to the host germline. PLOS Pathogens. 2007;3: 1930–1937. doi:10/c72vvk

20. Cooper BS, Ginsberg PS, Turelli M, Matute DR. *Wolbachia* in the *Drosophila yakuba* complex: pervasive frequency variation and weak cytoplasmic incompatibility, but no apparent effect on reproductive isolation. Genetics. 2017;205: 333–351. doi:10/f9s74s

21. Hoffmann AA, Turelli M, Simmons GM. Unidirectional incompatibility between populations of *Drosophila simulans*. Evolution. 1986;40: 692–701. doi:10/ggtgbg

22. Turelli M, Cooper BS, Richardson KM, Ginsberg PS, Peckenpaugh B, Antelope CX, et al. Rapid global spread of *w*Ri-like *Wolbachia* across multiple *Drosophila*. Current Biology. 2018;28: 963-971.e8. doi:10/gc3jdj

23. Turelli M, Hoffmann AA. Cytoplasmic incompatibility in *Drosophila simulans*: dynamics and parameter estimates from natural populations. Genetics. 1995;140: 1319–1338.

24. Hoffmann AA. Partial cytoplasmic incompatibility between two Australian populations of *Drosophila melanogaster*. Entomologia Experimentalis et Applicata. 1988;48: 61–67. doi:10/bthj43

25. Reynolds KT, Hoffmann AA. Male age, host effects and the weak expression or non-expression of cytoplasmic incompatibility in *Drosophila* strains infected by maternally transmitted *Wolbachia*. Genetical Research. 2002;80: 79–87.

26. Layton EM, On J, Perlmutter JI, Bordenstein SR, Shropshire JD. Paternal grandmother age affects the strength of *Wolbachia*-induced cytoplasmic incompatibility in *Drosophila melanogaster*. mBio. 2019;10. doi:10/gkbpjh

27. Early AM, Clark AG. Monophyly of *Wolbachia pipientis* genomes within *Drosophila melanogaster*: geographic structuring, titre variation and host effects across five populations. Molecular Ecology. 2013;22: 5765–5778. doi:10/f5hsgp

28. Hoffmann AA, Clancy DJ, Merton E. Cytoplasmic incompatibility in Australian populations of *Drosophila melanogaster*. Genetics. 1994;136: 993–999. doi:10/gkbpq6

29. Ilinsky YuYu, Zakharov IK. The endosymbiont *Wolbachia* in Eurasian populations of *Drosophila melanogaster*. Russian Journal of Genetics. 2007;43: 748. doi:10/bz3mv2

30. Kriesner P, Conner WR, Weeks AR, Turelli M, Hoffmann AA. Persistence of a *Wolbachia* infection frequency cline in *Drosophila melanogaster* and the possible role of reproductive dormancy. Evolution. 2016;70: 979–997. doi:10/f8tn6t

31. Webster CL, Waldron FM, Robertson S, Crowson D, Ferrari G, Quintana JF, et al. The Discovery, Distribution, and Evolution of Viruses Associated with *Drosophila melanogaster*. PLOS Biology. 2015;13: e1002210. doi:10/f7p96w

32. Hoffmann AA, Montgomery BL, Popovici J, Iturbe-Ormaetxe I, Johnson PH, Muzzi F, et al. Successful establishment of *Wolbachia* in *Aedes* populations to suppress dengue transmission. Nature. 2011;476: 454–457. doi:10/djxxp3

33. Ross PA, Axford JK, Yang Q, Staunton KM, Ritchie SA, Richardson KM, et al. Heatwaves cause fluctuations in *w*Mel *Wolbachia* densities and frequencies in *Aedes aegypti*. PLOS Neglected Tropical Diseases. 2020;14: e0007958. doi:10/gkbpm5

34. Ross PA, Ritchie SA, Axford JK, Hoffmann AA. Loss of cytoplasmic incompatibility in *Wolbachia*-infected *Aedes aegypti* under field conditions. PLOS Neglected Tropical Diseases. 2019;13: e0007357. doi:10/gkbpkq

35. Walker T, Johnson PH, Moreira LA, Iturbe-Ormaetxe I, Frentiu FD, McMeniman CJ, et al. The *w*Mel *Wolbachia* strain blocks dengue and invades caged *Aedes aegypti* populations. Nature. 2011;476: 450–453. doi:10/b8r6hf

36. Dobson SL, Fox Charles W., Jiggins Francis M. The effect of *Wolbachia*-induced cytoplasmic incompatibility on host population size in natural and manipulated systems. Proceedings of the Royal Society of London Series B: Biological Sciences. 2002;269: 437–445. doi:10/cvh466

37. Lees RS, Gilles JR, Hendrichs J, Vreysen MJ, Bourtzis K. Back to the future: the sterile insect technique against mosquito disease vectors. Current Opinion in Insect Science. 2015;10: 156–162. doi:10/gfq97f

38. Nikolouli K, Colinet H, Renault D, Enriquez T, Mouton L, Gibert P, et al. Sterile insect technique and *Wolbachia* symbiosis as potential tools for the control of the invasive species *Drosophila suzukii*. Journal of Pest Science. 2018;91: 489–503. doi:10/gc55cr

39. O'Connor L, Plichart C, Sang AC, Brelsfoard CL, Bossin HC, Dobson SL. Open release of male mosquitoes infected with a *Wolbachia* biopesticide: field performance and infection containment. PLOS Neglected Tropical Diseases. 2012;6: e1797. doi:10/f4dkm8

40. Crawford JE, Clarke DW, Criswell V, Desnoyer M, Cornel D, Deegan B, et al. Efficient production of male *Wolbachia*-infected *Aedes aegypti* mosquitoes enables large-scale suppression of wild populations. Nature Biotechnology. 2020;38: 482–492. doi:10/gkbppt

41. O'Neill SL. The use of *Wolbachia* by the World Mosquito Program to interrupt transmission of *Aedes aegypti* transmitted viruses. Advances in Experimental Medicine and Biology. 2018;1062: 355–360. doi:10/gkbpfk

42. O'Neill SL, Ryan PA, Turley AP, Wilson G, Retzki K, Iturbe-Ormaetxe I, et al. Scaled deployment of *Wolbachia* to protect the community from dengue and other *Aedes* transmitted arboviruses. Gates Open Research. 2018;2: 36. doi:10/ggh46h

43. Breeuwer JA, Werren JH. Cytoplasmic incompatibility and bacterial density in *Nasonia vitripennis*. Genetics. 1993;135: 565–574.

44. Clark ME, Veneti Z, Bourtzis K, Karr TL. *Wolbachia* distribution and cytoplasmic incompatibility during sperm development: the cyst as the basic cellular unit of CI expression. Mechanisms of Development. 2003;120: 185–198. doi:10/df2xdr

45. Veneti Z, Clark ME, Zabalou S, Karr TL, Savakis C, Bourtzis K. Cytoplasmic incompatibility and sperm cyst infection in different *Drosophila-Wolbachia* associations. Genetics. 2003;164: 545–552.

46. Bordenstein SR, Bordenstein SR. Temperature affects the tripartite interactions between bacteriophage WO, *Wolbachia*, and cytoplasmic incompatibility. PLOS One. 2011;6: e29106. doi:10/dbggwk

47. Foo IJ-H, Hoffmann AA, Ross PA. Cross-Generational Effects of Heat Stress on Fitness and *Wolbachia* Density in *Aedes aegypti* Mosquitoes. Tropical Medicine and Infectious Disease. 2019;4. doi:10/gkbpq9

48. Jia F-X, Yang M-S, Yang W-J, Wang J-J. Influence of continuous high temperature conditions on *Wolbachia* infection frequency and the fitness of *Liposcelis tricolor* (Psocoptera: Liposcelididae). Environmental Entomology. 2009;38: 1365–1372. doi:10/dqw5jh

49. Binnington KC, Hoffmann AA. *Wolbachia*-like organisms and cytoplasmic incompatibility in *Drosophila simulans*. Journal of Invertebrate Pathology. 1989;54: 344–352. doi:10/b5thqd

50. Bressac C, Rousset F. The Reproductive Incompatibility System in *Drosophila simulans*: DAPI-Staining Analysis of the *Wolbachia* Symbionts in Sperm Cysts. Journal of Invertebrate Pathology. 1993;61: 226–230. doi:10/c8hgvj

51. Clark ME, Veneti Z, Bourtzis K, Karr TL. The distribution and proliferation of the intracellular bacteria *Wolbachia* during spermatogenesis in *Drosophila*. Mechanisms of Development. 2002;111: 3–15. doi:10/dbhf9m

52. Karr TL, Yang W, Feder ME. Overcoming cytoplasmic incompatibility in *Drosophila*. Proceedings of the Royal Society B: Biological Sciences. 1998;265: 391–395. doi:10/dfzj8m

53. LePage DP, Metcalf JA, Bordenstein SR, On J, Perlmutter JI, Shropshire JD, et al. Prophage WO genes recapitulate and enhance *Wolbachi*a-induced cytoplasmic incompatibility. Nature. 2017;543: 243–247. doi:10/f9s35z

54. Beckmann J, Ronau JA, Hochstrasser M. A *Wolbachia* deubiquitylating enzyme induces cytoplasmic incompatibility. Nature Microbiology. 2017;2: 17007. doi:10/f9s5m7

55. Chen H, Ronau JA, Beckmann J, Hochstrasser M. A *Wolbachia* nuclease and its binding partner provide a distinct mechanism for cytoplasmic incompatibility. Proceedings of the National Academy of Sciences. 2019;116: 22314–22321. doi:10/gkbptp

56. Shropshire JD, Rosenberg R, Bordenstein SR. The impacts of cytoplasmic incompatibility factor (*cifA* and *cifB*) genetic variation on phenotypes. Genetics. 2021;217: 1–13. doi:10/gkbpfv

57. Shropshire JD, Bordenstein SR. Two-by-one model of cytoplasmic incompatibility: synthetic recapitulation by transgenic expression of *cifA* and *cifB* in *Drosophila*. PLOS Genetics. 2019;15: e1008221. doi:10/gkbpdw

58. Shropshire JD, On J, Layton EM, Zhou H, Bordenstein SR. One prophage WO gene rescues cytoplasmic incompatibility in *Drosophila melanogaster*. Proceedings of the National Academy of Sciences. 2018;115: 4987–4991. doi:10/gdcdff

59. Nasehi SF, Fathipour Y, Asgari S, Mehrabadi M. Environmental Temperature, but Not Male Age, Affects *Wolbachia* and Prophage WO Thereby Modulating Cytoplasmic Incompatibility in the Parasitoid Wasp, *Habrobracon Hebetor*. Microbial Ecology. 2021. doi:10/gjxss6

60. Bordenstein SR, Marshall ML, Fry AJ, Kim U, Wernegreen JJ. The tripartite associations between bacteriophage, *Wolbachia*, and arthropods. PLOS Pathogens. 2006;2: 384–393. doi:10/cht4w8

61. Masui S, Kamoda S, Sasaki T, Ishikawa H. Distribution and evolution of bacteriophage WO in *Wolbachia*, the endosymbiont causing sexual alterations in arthropods. Journal of Molecular Evolution. 2000;51: 491–497. doi:10/bx9ngt

62. Wright J, Sjostrand F, Portaro J, Barr A. Ultrastructure of Rickettsia-like microorganism *Wolbachia pipientis* and associated virus-like bodies in mosquito *Culex pipiens*. Journal of Ultrastructure Research. 1978;63: 79–85. doi:10/bsrtxv

63. Chrostek E, Marialva MSP, Esteves SS, Weinert LA, Martinez J, Jiggins FM, et al. *Wolbachia* variants induce differential protection to viruses in *Drosophila melanogaster*: a phenotypic and phylogenomic analysis. PLOS Genetics. 2013;9: e1003896. doi:10/f5qbgk

64. Duarte EH, Carvalho A, Lopez-Madrigal S, Teixeira L. Regulation of *Wolbachia* proliferation by the amplification and deletion of an addictive genomic island. bioRxiv. 2020; 2020.09.08.288217. doi:10/gkbphn

65. Hornett EA, Charlat S, Duplouy AMR, Davies N, Roderick GK, Wedell N, et al. Evolution of Male-Killer Suppression in a Natural Population. PLOS Biology. 2006;4: e283. doi:10/d4pwk4

66. Vanthournout B, Hendrickx F. Hidden suppression of sex ratio distortion suggests Red queen dynamics between *Wolbachia* and its dwarf spider host. Journal of Evolutionary Biology. 2016;29: 1488–1494. doi:10/f82pk6

67. Poinsot D, Bourtzis K, Markakis G, Savakis C, Mercot H. *Wolbachia* transfer from *Drosophila melanogaster* into *D. simulans*: Host effect and cytoplasmic incompatibility relationships. Genetics. 1998;150: 227–237. doi:10/gkbpvv

68. Funkhouser-Jones LJ, Opstal EJ van, Sharma A, Bordenstein SR. The Maternal Effect Gene *Wds* Controls *Wolbachia* Titer in *Nasonia*. Current Biology. 2018;0. doi:10/gdg6rg

69. Lu P, Bian G, Pan X, Xi Z. *Wolbachia* induces density-dependent inhibition to dengue virus in mosquito cells. PLOS Neglected Tropical Diseases. 2012;6: e1754. doi:10/f3469r

70. Awrahman ZA, Champion de Crespigny F, Wedell N. The impact of *Wolbachia*, male age and mating history on cytoplasmic incompatibility and sperm transfer in *Drosophila simulans*. Journal of Evolutionary Biology. 2014;27: 1–10. doi:10/f5m9sn

71. De Crespigny FEC, Pitt TD, Wedell N. Increased male mating rate in *Drosophila* is associated with *Wolbachia* infection. Journal of Evolutionary Biology. 2006;19: 1964–1972. doi:10/cgkd5x

72. Yamada R, Floate KD, Riegler M, O'Neill SL. Male development time influences the strength of *Wolbachia*-induced cytoplasmic incompatibility expression in *Drosophila melanogaster*. Genetics. 2007;177: 801–808. doi:10/fc8mmh

73. Clancy DJ, Hoffmann AA. Environmental effects on cytoplasmic incompatibility and bacterial load in *Wolbachia*-infected *Drosophila simulans*. Entomologia Experimentalis et Applicata. 1998;86: 13–24. doi:10/c8rj52

74. Meany MK, Conner WR, Richter SV, Bailey JA, Turelli M, Cooper BS. Loss of cytoplasmic incompatibility and minimal fecundity effects explain relatively low *Wolbachia* frequencies in *Drosophila mauritiana*. Evolution. 2019 [cited 16 Aug 2019]. doi:10/gkbpks

75. Kern AD, Barbash DA, Chang Mell J, Hupalo D, Jensen A. Highly constrained intergenic *Drosophila* ultraconserved elements are candidate ncRNAs. Genome Biology and Evolution. 2015;7: 689–698. doi:10/f7c4v8

76. Lindsey A, Rice DW, Bordenstein SR, Brooks AW, Bordenstein SR, Newton ILG. Evolutionary genetics of cytoplasmic incompatibility genes *cifA* and *cifB* in prophage WO of *Wolbachia*. Genome Biology and Evolution. 2018;10: 434–451. doi:10/gcvmkm

77. Bing X-L, Zhao D-S, Sun J-T, Zhang K-J, Hong X-Y. Genomic analysis of *Wolbachia* from *Laodelphax striatellus* (Delphacidae, Hemiptera) reveals insights into its "Jekyll and Hyde" mode of infection pattern. Genome Biology and Evolution. 2020. doi:10/gkbpnf

78. Martinez J, Klasson L, Welch JJ, Jiggins FM. Life and death of selfish genes: comparative genomics reveals the dynamic evolution of cytoplasmic incompatibility. Molecular Biology and Evolution. 2020. doi:10/gjfqg8

79. Bordenstein SR, Bordenstein SR. Eukaryotic association module in phage WO genomes from *Wolbachia*. Nature Communications. 2016;7: 13155. doi:10/f87pxk

80. Chrostek E, Teixeira L. Mutualism breakdown by amplification of *Wolbachia* genes. PLOS Biology. 2015;13: e1002065. doi:10/f635j3

81. Myllymäki H, Valanne S, Rämet M. The *Drosophila* Imd Signaling Pathway. The Journal of Immunology. 2014;192: 3455–3462. doi:10/f5xwg8

82. Clark ME, Karr TL. Distribution of *Wolbachia* within *Drosophila* reproductive tissue: implications for the expression of cytoplasmic incompatibility. Integrative and comparative biology. 2002;42: 332–339. doi:10/dh49bd

83. Doremus MR, Stouthamer CM, Kelly SE, Schmitz-Esser S, Hunter MS. *Cardinium* Localization During Its Parasitoid Wasp Host's Development Provides Insights Into Cytoplasmic Incompatibility. Frontiers in Microbiology. 2020;11. doi:10/gkbpr9

84. Doremus MR, Kelly SE, Hunter MS. Exposure to opposing temperature extremes causes comparable effects on *Cardinium* density but contrasting effects on *Cardinium*-induced cytoplasmic incompatibility. PLOS Pathogens. 2019;15: e1008022. doi:10/gkbppb

85. Graveley BR, Brooks AN, Carlson JW, Duff MO, Landolin JM, Yang L, et al. The Developmental Transcriptome of *Drosophila melanogaster*. Nature. 2011;471: 473–479. doi:10/dzqgmd

86. Kaur R, Martinez J, Rota-Stabelli O, Jiggins FM, Miller WJ. Age, tissue, genotype and virus infection regulate *Wolbachia* levels in *Drosophila*. Molecular Ecology. 2020;29. doi:10/ghfj5g

87. Hotopp JCD, Lin M, Madupu R, Crabtree J, Angiuoli SV, Eisen J, et al. Comparative Genomics of Emerging Human Ehrlichiosis Agents. PLOS Genetics. 2006;2: e21. doi:10/fmsmgs

88. Vollmer J, Schiefer A, Schneider T, Jülicher K, Johnston KL, Taylor MJ, et al. Requirement of lipid II biosynthesis for cell division in cell wall-less *Wolbachia*, endobacteria of arthropods and filarial nematodes. International journal of medical microbiology: IJMM. 2013;303: 140–149. doi:10/f4smsf

89. Louis C, Nigro L. Ultrastructural evidence of *Wolbachia* rickettsiales in *Drosophila simulans* and their relationships with unidirectional cross-incompatibility. Journal of Invertebrate Pathology. 1989;54: 39–44. doi:10/cj75mb

90. Bian G, Xu Y, Lu P, Xie Y, Xi Z. The endosymbiotic bacterium *Wolbachia* induces resistance to dengue virus in *Aedes aegypti*. PLOS Pathogens. 2010;6: e1000833. doi:10/d33jr5

91. Kambris Z, Cook PE, Phuc HK, Sinkins SP. Immune activation by life-shortening *Wolbachia* and reduced filarial competence in mosquitoes. Science. 2009;326: 134–136. doi:10/bwf6sx

92. Moreira LA, Iturbe-Ormaetxe I, Jeffery JA, Lu G, Pyke AT, Hedges LM, et al. A *Wolbachia* symbiont in *Aedes aegypti* limits infection with dengue, Chikungunya, and Plasmodium. Cell. 2009;139: 1268–1278. doi:10/c2jm62

93. Xi Z, Gavotte L, Xie Y, Dobson SL. Genome-wide analysis of the interaction between the endosymbiotic bacterium *Wolbachia* and its *Drosophila* host. BMC Genomics. 2008;9: 1. doi:10/bb6h53

94. Bourtzis K, Pettigrew MM, O'Neill SL. *Wolbachia* neither induces nor suppresses transcripts encoding antimicrobial peptides. Insect molecular biology. 2000;9: 635–639.

95. Rancès E, Johnson TK, Popovici J, Iturbe-Ormaetxe I, Zakir T, Warr CG, et al. The toll and Imd pathways are not required for *Wolbachia*-mediated dengue virus interference. Journal of Virology. 2013;87: 11945–11949. doi:10/gkbpfn

96. Wong ZS, Hedges LM, Brownlie JC, Johnson KN. *Wolbachia*-mediated antibacterial protection and immune gene regulation in *Drosophila*. PLOS One. 2011;6: e25430. doi:10/bdfqsh

97. Zhang Y-K, Ding X-L, Rong X, Hong X-Y. How do hosts react to endosymbionts? A new insight into the molecular mechanisms underlying the *Wolbachia*-host association. Insect Molecular Biology. 2015;24: 1–12. doi:10/f6wjxc

98. Broderick NA, Buchon N, Lemaitre B. Microbiota-induced changes in *Drosophila melanogaster* host gene expression and gut morphology. mBio. 2014;5: e01117-01114. doi:10/ghkqnf

99. Buchon N, Broderick NA, Chakrabarti S, Lemaitre B. Invasive and indigenous microbiota impact intestinal stem cell activity through multiple pathways in *Drosophila*. Genes & Development. 2009;23: 2333–2344. doi:10/bhdwhb

100. Guo L, Karpac J, Tran SL, Jasper H. PGRP-SC2 promotes gut immune homeostasis to limit commensal dysbiosis and extend lifespan. Cell. 2014;156: 109–122. doi:10/f5pkm9

101. Ha E-M, Lee K-A, Park SH, Kim S-H, Nam H-J, Lee H-Y, et al. Regulation of DUOX by the Galphaq-phospholipase Cbeta-Ca2+ pathway in *Drosophila* gut immunity. Developmental Cell. 2009;16: 386–397. doi:10/b46996

102. Landis GN, Abdueva D, Skvortsov D, Yang J, Rabin BE, Carrick J, et al. Similar gene expression patterns characterize aging and oxidative stress in *Drosophila melanogaster*. Proceedings of the National Academy of Sciences. 2004;101: 7663–7668. doi:10/dzgsxw

103. Pletcher SD, Macdonald SJ, Marguerie R, Certa U, Stearns SC, Goldstein DB, et al. Genome-Wide Transcript Profiles in Aging and Calorically Restricted *Drosophila melanogaster*. Current Biology. 2002;12: 712–723. doi:10/fpjg2k

104. Seroude L, Brummel T, Kapahi P, Benzer S. Spatio-temporal analysis of gene expression during aging in *Drosophila melanogaster*. Aging Cell. 2002;1: 47–56. doi:10/bth6sv

105. Clark RI, Salazar A, Yamada R, Fitz-Gibbon S, Morselli M, Alcaraz J, et al. Distinct Shifts in Microbiota Composition during *Drosophila* Aging Impair Intestinal Function and Drive Mortality. Cell Reports. 2015;12: 1656–1667. doi:10/gkbpqm

106. Mistry R, Kounatidis I, Ligoxygakis P. Interaction Between Familial Transmission and a Constitutively Active Immune System Shapes Gut Microbiota in *Drosophila melanogaster*. Genetics. 2017;206: 889–904. doi:10/gbh694

107. Ren C, Webster P, Finkel SE, Tower J. Increased Internal and External Bacterial Load during *Drosophila* Aging without Life-Span Trade-Off. Cell Metabolism. 2007;6: 144–152. doi:10/bmqhnb

108. Buchon N, Silverman N, Cherry S. Immunity in *Drosophila melanogaster*--from microbial recognition to whole-organism physiology. Nature Reviews Immunology. 2014;14: 796–810. doi:10/f6qs8g

109. Hoffmann AA, Hercus M, Dagher H. Population dynamics of the *Wolbachia* infection causing cytoplasmic incompatibility in *Drosophila melanogaster*. Genetics. 1998;148: 221–231. doi:10/gkbpjd

110. Schuler H, Köppler K, Daxböck-Horvath S, Rasool B, Krumböck S, Schwarz D, et al. The hitchhiker's guide to Europe: the infection dynamics of an ongoing *Wolbachia* invasion and mitochondrial selective sweep in *Rhagoletis cerasi*. Molecular Ecology. 2016;25: 1595–1609. doi:10/f3s255

111. Wheeler TB, Thompson V, Conner WR, Cooper BS. *Wolbachia* in the spittlebug *Prosapia ignipectus*: Variable infection frequencies, but no apparent effect on host reproductive isolation. bioRxiv. 2021; 2021.02.25.432892. doi:10/gkbpc6

112. Cooper BS, Vanderpool D, Conner WR, Matute DR, Turelli M. *Wolbachia* acquisition by *Drosophila yakuba*-clade hosts and transfer of incompatibility loci between distantly related *Wolbachia*. Genetics. 2019. doi:10/ggh6t7

113. Ballard JWO, Melvin RG. Tetracycline treatment influences mitochondrial metabolism and mtDNA density two generations after treatment in *Drosophila*. Insect Molecular Biology. 2007;16: 799–802. doi:10/fprwnc

114. Kõressaar T, Lepamets M, Kaplinski L, Raime K, Andreson R, Remm M. Primer3_masker: integrating masking of template sequence with primer design software. Bioinformatics. 2018;34: 1937–1938. doi:10/gdmgg8

115. Hu Y, Sopko R, Foos M, Kelley C, Flockhart I, Ammeux N, et al. FlyPrimerBank: an online database for *Drosophila melanogaster* gene expression analysis and knockdown evaluation of RNAi reagents. G3. 2013;3: 1607–1616. doi:10/gkbpnt

116. Hu Y, Comjean A, Perrimon N, Mohr S. The *Drosophila* Gene Expression Tool (DGET) for expression analyses. BMC Bioinformatics. 2017;18: 98. doi:10/gkbpf4

117. R Core Team. R: A Language and Environment for Statistical Computing. Vienna, Austria: R Foundation for Statistical Computing; 2020. Available: https://www.R-project.org/

118. Kassambara A. ggpubr: "ggplot2" Based Publication Ready Plots. 2020. Available: https://CRAN.R-project.org/package=ggpubr

119. Signorell A. Tools for Descriptive Statistics [R package DescTools version 0.99.41]. Comprehensive R Archive Network (CRAN); 2021. Available: https://CRAN.R-project.org/package=DescTools

120. Canty A, Ripley BD. boot: Bootstrap R (S-Plus) Functions. 2021.

121. Wickham H. ggplot2: Elegant Graphics for Data Analysis. Springer-Verlag New York; 2016. Available: https://ggplot2.tidyverse.org

1042

1043 **Supporting Information**

1044

1045

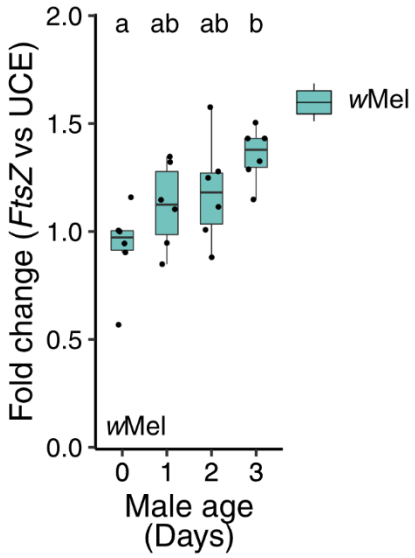

1046

1047 **Figure S1. Testing the bacterial density model for CI strength variation in young *w*Mel-**
1048 **infected *D. melanogaster*.** Fold change across male age for *w*Mel *FtsZ* relative to *D.*
1049 *melanogaster* UCE. Letters above data represent statistically significant differences based on
1050 α=0.05 calculated by Kruskal-Wallis and Dunn's test for multiple comparisons between all
1051 groups—crosses that do not share a letter are significantly different. Fold change was
1052 calculated as $2^{-\Delta\Delta cq}$. *P*-values are reported in Table S1.

1053

1054

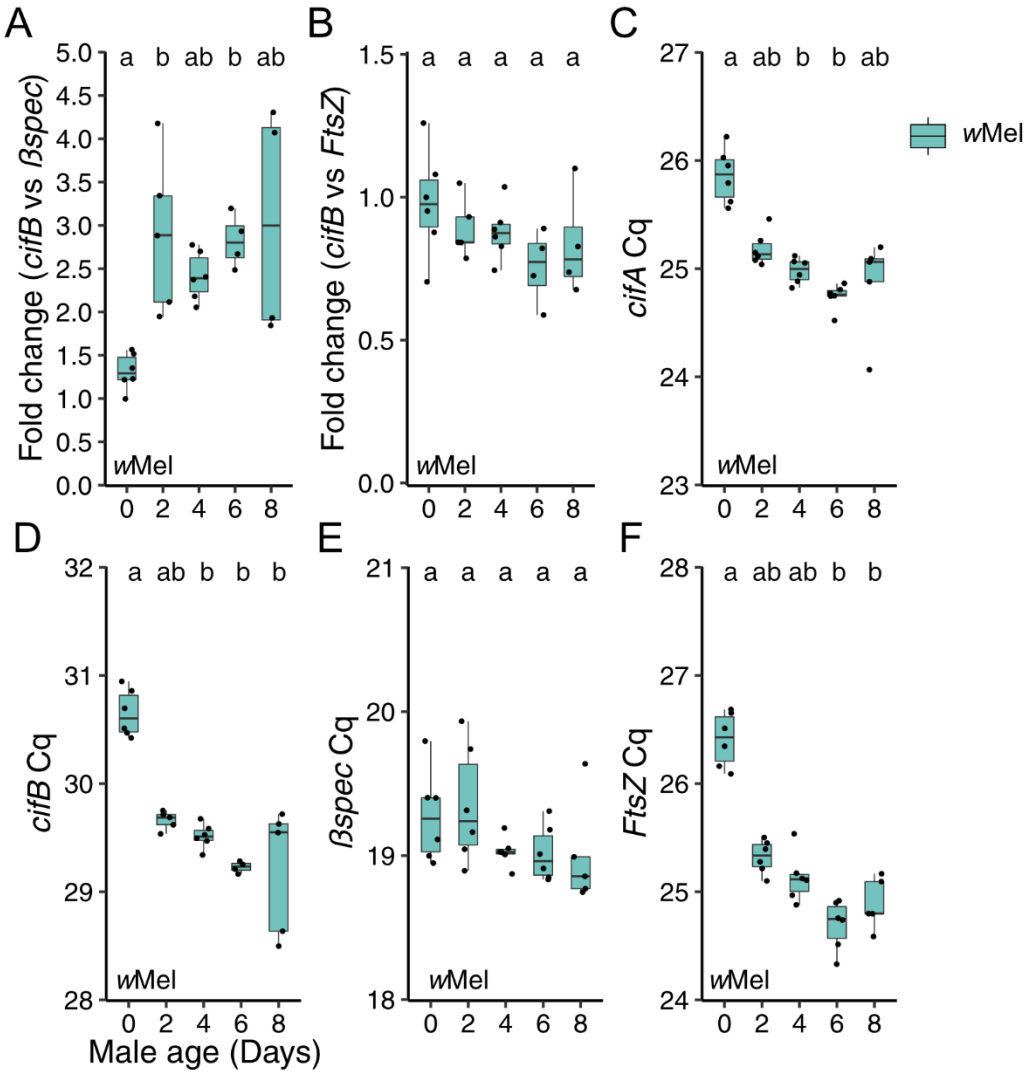

Figure S2. Testing the *cif* expression hypothesis for *w*Mel CI strength variation. Fold change across male age for the relative expression of (A) $cifB_{wMel[T1]}$ to *D. melanogaster βspec* and (B) $cifB_{wMel[T1]}$ to *w*Mel *FtsZ*. Raw C_q values for (C) $cifA_{wMel[T1]}$, (D) $cifB_{wMel[T1]}$, (E) *D. melanogaster βspec*, and (D) *w*Mel *FtsZ*. Letters above data represent statistically significant differences based on α=0.05 calculated by Kruskal-Wallis and Dunn's test for multiple comparisons between all groups—crosses that do not share a letter are significantly different. Fold change was calculated as $2^{-\Delta\Delta cq}$. *P*-values are reported in Table S1.

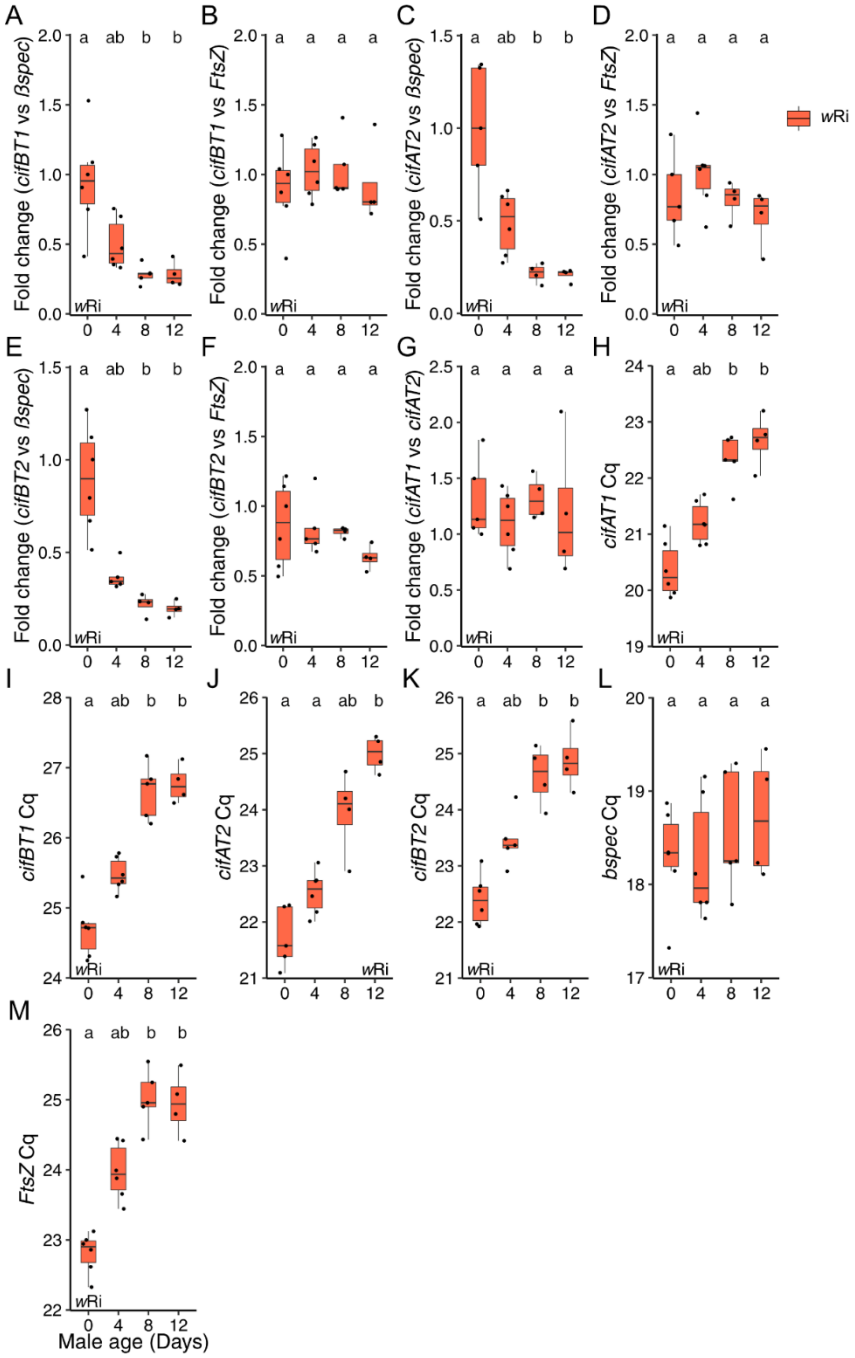

Figure S3. Testing the *cif* expression hypothesis for *w*Ri CI strength variation. Fold change across male age for the relative expression of (A) $cifB_{wRi[T1]}$ to *D. simulans βspec*, (B) $cifB_{wRi[T1]}$ to *w*Ri *FtsZ*, (C) $cifA_{wRi[T2]}$ to *D. simulans βspec*, (D) $cifA_{wRi[T2]}$ to *w*Ri *FtsZ*, (E) $cifB_{wRi[T2]}$ to *D. simulans βspec*, (F) $cifB_{wRi[T2]}$ to *w*Ri *FtsZ*, and (G) $cifA_{wRi[T1]}$ to $cifA_{wRi[T2]}$. Raw C_q values for (H) $cifA_{wRi[T1]}$, (I) $cifB_{wRi[T1]}$, (J) $cifA_{wRi[T2]}$, (K) $cifB_{wRi[T2]}$, (L) *D. simulans βspec*, and (M) *w*Ri *FtsZ*. Letters above data represent statistically significant differences based on α=0.05 calculated by Kruskal-Wallis and Dunn's test for multiple comparisons between all groups—crosses that do

not share a letter are significantly different. Fold change was calculated as $2^{-\Delta\Delta cq}$. *P*-values are reported in Table S1.

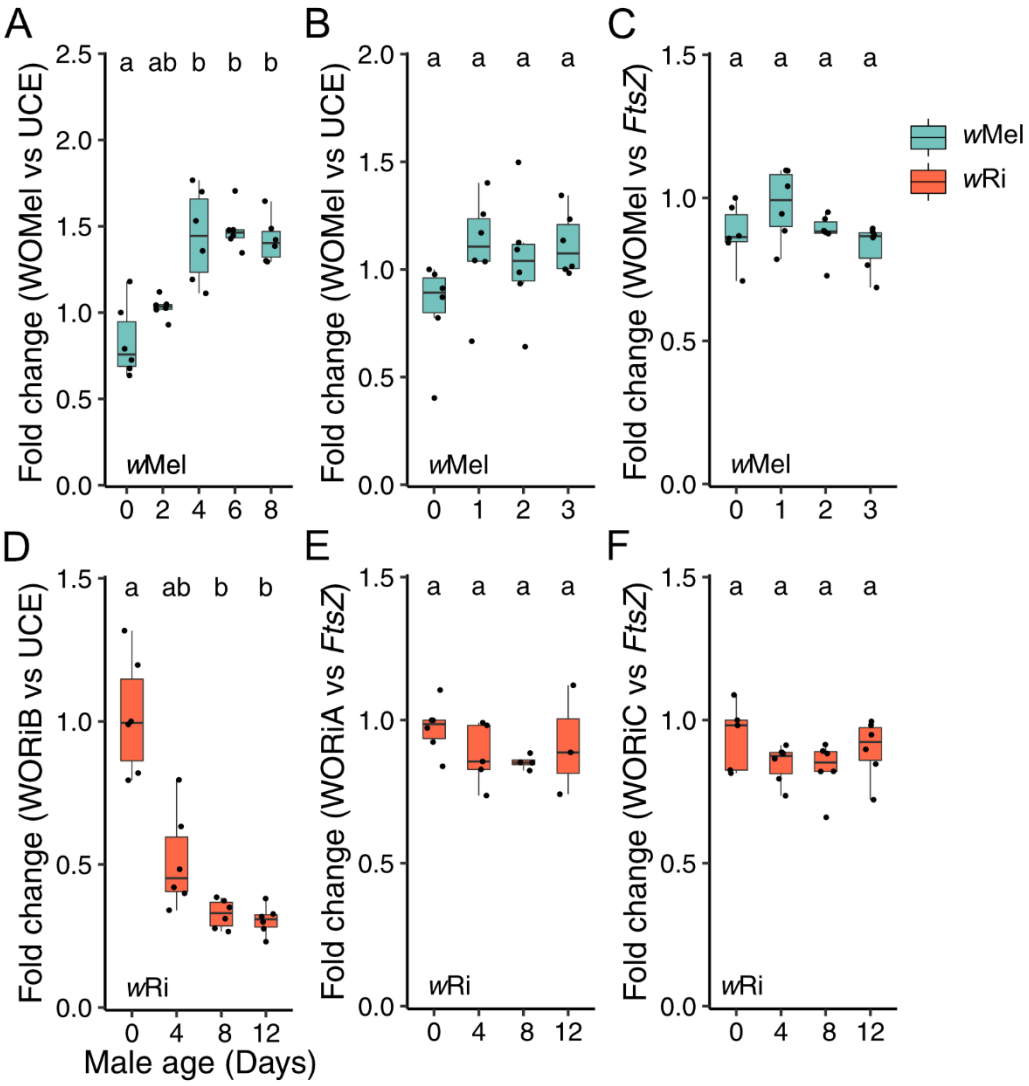

Figure S4. Testing the phage density model for *Wolbachia* density variation. Fold change across male age for the relative abundance of (A) WOMelA/B to *D. melanogaster* UCE in the old age cohort, (B) WOMelA/B to *D. melanogaster* UCE in the young age cohort, (C) WOMelA/B to *w*Mel *FtsZ* in the young age cohort, (D) WORiB to *D. simulans* UCE, (E) WORiA to *w*Ri *FtsZ*, and (F) WORiC to *w*Ri *FtsZ*. Letters above data represent statistically significant differences based on α=0.05 calculated by Kruskal-Wallis and Dunn's test for multiple comparisons between all groups—crosses that do not share a letter are significantly different. Fold change was calculated as $2^{-\Delta\Delta cq}$. *P*-values are reported in Table S1.

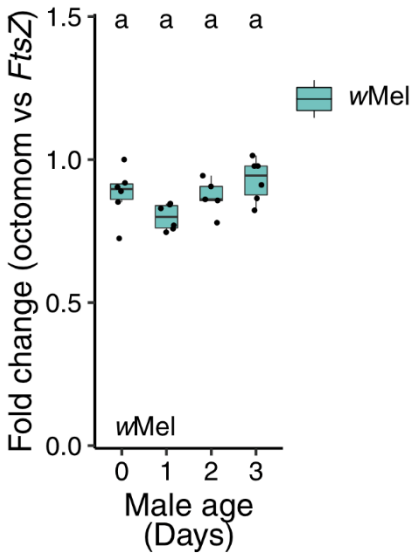

Figure S5. Testing the Octomom copy number hypothesis for *w*Mel density variation in young *w*Mel-infected *D. melanogaster*. Fold change across male age for the relative abundance of Octomom gene WD0509 to *w*Mel *FtsZ* in the young cohort. Letters above data represent statistically significant differences based on α=0.05 calculated by Kruskal-Wallis and Dunn's test for multiple comparisons between all groups—crosses that do not share a letter are significantly different. Fold change was calculated as $2^{-\Delta\Delta cq}$. *P*-values are reported in Table S1.